JCTC Journal of Chemical Theory and Computation

Article

pubs.acs.org/JCTC

Molecular Dynamics Investigation of Alkali Metal Ions in Liquid and Aqueous Ammonia

Esam A. Orabi[†] and Guillaume Lamoureux*

Department of Chemistry and Biochemistry and Centre for Research in Molecular Modeling (CERMM), Concordia University, 7141 Sherbrooke Street West, Montréal, Québec H4B 1R6, Canada

ABSTRACT: A polarizable potential model for M^+–NH_3 interactions (M^+ = Li^+, Na^+, K^+, Rb^+, Cs^+) is optimized based on the ab initio properties of the ion–ammonia dimers calculated at the MP2 level of theory. The optimized model reproduces the ab initio binding energies of $M^+(NH_3)_n$ (n = 2–4) and $M^+(NH_3)_n(H_2O)_m$ (n, m = 1–3 and $n + m \leq 4$) clusters and gives relative solvation free energies in liquid ammonia in good agreement with experimental data, without further adjustments. It also reproduces binding cooperativity in ion–ammonia and ion–ammonia–water clusters. The model is used in molecular dynamics simulations of isolated ions in liquid ammonia and in aqueous ammonia solutions with various ammonia molar fractions ($0.0 \leq x_{NH_3} \leq 1.0$). Simulations in liquid ammonia show coordination numbers of 4.0 for Li^+, 5.3 for Na^+, 6.1 for K^+, 6.7 for Rb^+, and 7.7 for Cs^+, in very good agreement with available experimental results. Simulations of ions in aqueous ammonia show preferential solvation by water in their first solvation shells and preferential solvation by ammonia in their second shells. Potentials of mean force are calculated between each ion and NH_3 in liquid water, and between each ion and H_2O in liquid ammonia. The results suggest that, in liquid water, Li^+ and Na^+ bind NH_3 in their second solvation shells only, while Cs^+ binds NH_3 in its first solvation shell only (K^+ and Rb^+ ions show only weak affinity for NH_3 in water). In liquid ammonia, the ions bind H_2O in their first solvation shells with an affinity following the trend $Li^+ > Na^+ > K^+ \approx Rb^+ > Cs^+$.

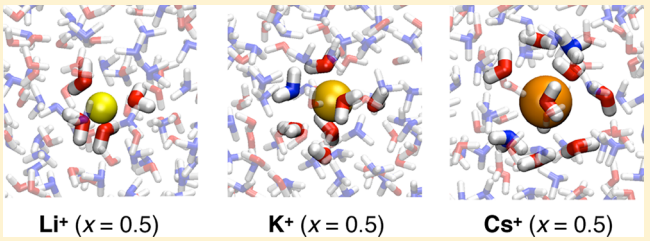

1. INTRODUCTION

Ammonia is a good solvent for many metals, nonmetals, and electrolytes and has a widespread use in many industrial sectors.[1] Alkali metals dissolve in anhydrous ammonia through dissociation into positive metal ions and free electrons.[1,2] The conductivity of alkali ions in liquid ammonia increases with concentration of the metal.[2] At low concentrations, the solutions are nonmetallic and blue-colored (a hallmark of solvated electrons), but they become metallic and bronze-colored at high concentrations. The dissolution of alkali metals in liquid ammonia is also characterized by a decrease in the density of the solution with the metal concentration.[2−4] At high metal concentrations, the density of the solution is markedly lower than that of either of its components.[2−4] The unusual electric and volumetric properties of these solutions have been the subject of various experimental[5−10] and theoretical investigations.[11−28] While electrons must be treated as quantum particles, in dilute solutions the alkali metal cores are decoupled from the free electrons and can be investigated using classical simulations.[11−14,16−18,20,22]

Solvation of alkali ions in liquid ammonia has been the subject of various computational approaches such as quantum path integral Monte Carlo (PIMC),[12] hybrid quantum mechanics/molecular mechanics (QM/MM),[15,20] classical Monte Carlo (MC),[12,17,18] and molecular dynamics (MD)[11,13,14,16,22] simulations. However, few of these theoretical investigations have shown consistent agreement with experimental data. For instance, simulations of Li^+ in liquid ammonia have yielded first-shell coordination numbers of either 4[12,15,24] or 6,[11,14,15,18,22] compared to the experimentally reported tetrahedral arrangement of four NH_3 molecules.[6,7,9] Coordination numbers of 5,[12,20] 7,[13] 8,[13,17,20] and 9[17] have been reported for Na^+, compared to the experimental coordination number of ∼5.5.[6] Using MD simulations, Tongraar et al.[16] have reported a coordination number of 8.7 for K^+, which seems overestimated since the experimental coordination number reported for the larger Rb^+ ion is 6.4 NH_3 molecules.[8] Using classical MC simulations, Marchi et al.[12] have reported a coordination number of 10 for Cs^+ in liquid ammonia at 260 K, which again seems overestimated. Although some of the reported potential models have shown agreement with experimental results (especially for Li^+), none have been used to systematically study the solvation of the whole alkali series. Even with the computationally expensive QM/MM simulations, the coordination number and the solvation structure have been observed to depend on the level of theory used to treat the QM region. For instance, Tongraar and Hannongbua[29] have studied the solvation structure of NH_4^+ and reported a coordination number of 5.1 from QM(HF)/MM simulations and of 4.3 from QM(B3LYP)/MM simulations.

While the majority of published theoretical studies focus on metal ions in pure solvents, the solvation of alkali ions in liquid mixtures has received less attention.[30−36] Such studies are important to elucidate the phenomenon of preferential solvation, which plays an important role in the solubility of ions in mixed solvents and in understanding ion–ligand binding selectivity. Preferential solvation of the alkali ions Li^+, Na^+, and K^+ in 18.4%

Received: February 8, 2013
Published: April 30, 2013

   dx.doi.org/10.1021/ct4001069 | J. Chem. Theory Comput. 2013, 9, 2324−2338

NH_3 (mole fraction) has been studied by classical MC and MD techniques[30−34] and by QM/MM simulations.[32−35] The solvation of a Li atom in 25 water molecules and 6 ammonia molecules (19.4% NH_3) has also been studied by first-principles Car−Parrinello molecular dynamics simulations.[36] At 18.4% NH_3 mole fraction, classical simulations have suggested the following first solvation shell structures: $Li^+(H_2O)_4(NH_3)_2$,[31] $Li^+(H_2O)_3(NH_3)_3$,[32] $Na^+(H_2O)_{2.4}(NH_3)_4$,[30] $Na^+(H_2O)_{4.9}(NH_3)_{2.2}$,[33] and $K^+(H_2O)_{5.3}(NH_3)_{3.4}$.[34] QM/MM simulations from Tongraar and Rode show different structures: $Li^+(H_2O)_3(NH_3)$,[32] $Li^+(H_2O)_4$,[35] $Na^+(H_2O)_{3.7}(NH_3)_{1.8}$,[33] and $K^+(H_2O)_{6.7}(NH_3)_{0.9}$.[34] Car−Parrinello MD simulations of a lithium atom in a 19.4% NH_3 solution show spontaneous ionization of Li and a first solvation shell structure $Li^+(H_2O)_4$.[36] While the structures are different, the accuracy of the method cannot be determined unless experimental results are available.

Ab initio MD simulations can in principle provide a physically accurate picture of ions in solution and of hydrogen bonds between solvent molecules but may require a level of quantum theory that is not always amenable to extensive sampling. This is especially problematic for solvent mixtures in which the various components exchange in and out of the ion solvation shell at a slow rate. In contrast, force fields are computationally inexpensive and can be used for reliable sampling of the configuration space. They however do not represent electrons explicitly and often neglect polarization effects, which have been shown to contribute significantly to cation−ammonia interactions.[21,23] Ab initio energy decomposition analysis on the Li^+−NH_3 complex[21] has shown that polarization contributes to 16.3% of the total interaction energy—a fraction comparable to that of the Li^+−H_2O complex (19.9%).[37] Corral et al.[23] have similarly investigated the nature of binding of alkali and alkaline-earth cations with a series of oxygen and nitrogen ligands and found that polarization effects are important to reproduce the correct basicity trend. In addition, nonadditive terms may largely affect the simulation results of ion-containing solutions.[19,32−34]

In this work, we aim to develop a reliable polarizable potential model for alkali ion−ammonia interactions and investigate ion solvation in both pure and aqueous ammonia solutions. The model is optimized to reproduce the ab initio properties of ion−ammonia dimers (geometries, binding energies, and potential energy surfaces) calculated at the MP2 level. It is then validated using the ab initio binding energies of $M^+(NH_3)_n$ (n = 2−4) and $M^+(NH_3)_n(H_2O)_m$ (n, m = 1−3 and $n + m \leq 4$) clusters, and the solvation free energies of the ions in liquid ammonia. The model is used to investigate the solvation structure of the ions in liquid ammonia and, in combination with a model for ion−water interactions developed previously,[38,39] to investigate preferential solvation in aqueous ammonia solutions with various ammonia mole fractions ($0 \leq x_{NH_3} \leq 1$).

2. METHODS

2.1. Ab Initio Calculations. The structures of alkali ion−ammonia binary clusters, $M^+(NH_3)_n$ (n = 1−4), and alkali ion−ammonia−water ternary clusters, $M^+(NH_3)_n(H_2O)_m$ (n, m = 1−3 and $n + m \leq 4$), are optimized at the MP2 level of theory using Gaussian 09.[40] For complexes of Li^+, Na^+, and K^+, calculations are performed at the frozen core (FC) MP2/6-311++G(d,p) level and yield binding energies for the ion−ammonia dimers in very good agreement with experimental data. It should be noted that the MP2(FC) calculations yield binding energies for ion−ammonia dimers in close agreement with MP2(full) results. Complexes of the heavier alkali cations (Rb^+ and Cs^+) are calculated at the full-electron MP2 level with the 6-311+G(3df,2p) basis set for H, N, and O and with effective core potentials (ECPs) and valence basis sets for the metal ions. We use the Stuttgart RSC 1997 (ECP) basis set[41] to which d and f polarization functions are added with exponents 0.39 and 0.55 for Rb^+ and 0.29 and 0.44 for Cs^+.[42] The basis sets used to study Rb^+ and Cs^+ clusters were shown to give binding energies for the benzene−ion complexes in good agreement with experimental results.[42] They also yield ion−water binding energies in very good agreement with experimental results (see below). All calculations are done without symmetry constraints, and frequency calculations are performed on the resulting structures to confirm that they are energy minima. Interaction energies are corrected for basis set superposition error (BSSE) using the counterpoise (CP) procedure of Boys and Bernardi.[43] Potential energy surfaces (PESs) for the M^+−NH_3 dimers are generated by scanning the M^+···N distance from 1 to 8 Å and the M^+···N−H angle from 0 to 180°. The surfaces are computed using rigid ammonia geometry, calculated at the MP2(FC)/6-311++G(d,p) level (r_{NH} = 1.0135 Å and θ_{HNH} = 107.29°),[44] and are corrected for BSSE.

2.2. Molecular Mechanics Calculations. Molecular mechanics (MM) calculations are performed with the program CHARMM.[45] Polarizable potential models based on classical Drude oscillators[46] have been reported for H_2O,[38] alkali ions,[39] and NH_3.[44] The SWM4-NDP water model was calibrated to reproduce the main properties of liquid water, including the self-diffusion coefficient and dielectric constant.[38] The alkali cation model reproduces the experimental solvation structure and hydration free energies of the ions.[39] The ammonia model reproduces the properties of liquid, supercritical, and aqueous ammonia solutions.[44] Following our previous work,[44,47−49] a polarizable model for alkali ion−ammonia interactions is optimized on the basis of the ab initio properties of the ion−ammonia dimers.

2.2.1. Potential Energy Function and Parametrization Strategy. Molecular polarizability is described by attaching a light (0.4 amu), negatively charged "Drude" particle to all non-hydrogen atoms using a harmonic spring with force constant k_D = 1000 kcal/mol/Å^2.[46] The partial charge q_i of a polarizable atom i is then distributed between the Drude particle (q_{Di}) and the atomic core ($q_{ci} = q_i - q_{Di}$) with the Drude particle charge being determined from the atomic polarizability via the relation $\alpha_i = q_{Di}^2/k_D$. A displacement d between the Drude particle and the polarizable atom results in an induced dipole moment $q_{Di}d$. The polarizable potential energy function that describes the interaction energy in liquid and aqueous ammonia solutions containing alkali ions is given as[44,47]

$$U(R) = \sum_{i=1}^{N} \frac{1}{2} k_D |\mathbf{r}_{ci} - \mathbf{r}_{Di}|^2 + \sum_{\text{HNH angles}} k_\theta(\theta - \theta_0)^2 + \sum_{\text{nonbond}} E_{\min,ij}\left[\left(\frac{R_{\min,ij}}{|\mathbf{r}_{ci} - \mathbf{r}_{cj}|}\right)^{12} - 2\left(\frac{R_{\min,ij}}{|\mathbf{r}_{ci} - \mathbf{r}_{cj}|}\right)^{6}\right] + \sum_{\text{nonbond}} \left(\frac{q_{ci}q_{cj}}{|\mathbf{r}_{ci} - \mathbf{r}_{cj}|} + \frac{q_{ci}q_{Dj}}{|\mathbf{r}_{ci} - \mathbf{r}_{Dj}|} + \frac{q_{Di}q_{cj}}{|\mathbf{r}_{Di} - \mathbf{r}_{cj}|} + \frac{q_{Di}q_{Dj}}{|\mathbf{r}_{Di} - \mathbf{r}_{Dj}|}\right) \quad (1)$$

where N is the number of interacting molecules and $\mathbf{r}_{ci}$ and $\mathbf{r}_{Di}$ are positions of the core particle i and its Drude particle,

dx.doi.org/10.1021/ct4001069 | J. Chem. Theory Comput. 2013, 9, 2324−2338

respectively. k_θ and θ_0 are respectively the force constant and equilibrium angle for the HNH angles θ. $E_{\min,ij}$ and $R_{\min,ij}$ are the mixed Lennard-Jones (LJ) parameters between nonbonded atoms i and j, defined by the Lorentz−Berthelot combination rules:

$$E_{\min,ij} = \sqrt{E_{\min,i} \times E_{\min,j}} \text{ and } R_{\min,ij} = \frac{R_{\min,i} + R_{\min,j}}{2} \quad (2)$$

Equation 1 does not include bond stretching energy terms since for both water and ammonia, bonds are constrained to their equilibrium values using the SHAKE/Roll-RATTLE/Roll algorithm.[50] It also does not include HOH angle bending terms since the SWM4-NDP water model has a rigid molecular geometry.[38] A polarizable model for alkali ion−ammonia interactions is optimized following our previously reported approach.[44,47] In particular, pair-specific LJ parameters between each ion and the nitrogen atom of NH_3 are optimized based on the ab initio properties of the ion−ammonia dimers. Parameters are first optimized to reproduce the calculated ab initio PESs.[47] Since these PESs are calculated with rigid ammonia geometry, we further refine the obtained parameters to give complexation energies of the relaxed ion−ammonia dimers in agreement with the ab initio minimum energy structures.[44] (For the dimers calculated with the force field, the $M^+\cdots N$ distance and HNH angles are allowed to relax, but NH bonds are constrained at their equilibrium values.)

2.2.2. Molecular Dynamics. Simulations are performed with cubic periodic boundary conditions in the isothermal−isobaric ensemble (NpT). All MD simulations are performed at the normal boiling point of ammonia (T = 239.8 K and p = 1 atm), except those for calculating the solvation free energies of the ions, which are performed at T = 298.15 K and p = 9.9 atm (the corresponding vapor pressure of liquid ammonia). The water-rich solutions at 239.8 K remain in the supercooled state for the duration of all simulations. The total number of molecules (one ion + ammonia + water) is 251 in all simulations. Eleven ammonia mole fractions are simulated: x_{NH_3} = 0, 0.1, 0.2, 0.3, 0.4, 0.5, 0.6, 0.7, 0.8, 0.9, and 1 (calculated without considering the ion). Electrostatic interactions are computed using the particle-mesh Ewald method[51] with κ = 0.34 for the charge screening and a 1.0 Å grid spacing with fourth-order splines for the mesh interpolation. The real-space interactions (Lennard-Jones and electrostatic) are cut off at 15 Å, and the long-range contribution from the Lennard-Jones term is introduced as an average density-dependent term.[52] The temperature of the system is controlled with a two-thermostats algorithm, where atoms are kept at the desired temperature and oscillations of the Drude particles are kept at low temperature (1 K) to ensure self-consistent dipole induction.[46] The equations of motion are integrated using a 1 fs time step, with all bonds involving hydrogen atoms kept at their reference lengths using the SHAKE/Roll and RATTLE/Roll algorithms.[50] Simulations in liquid ammonia are run for 20 ns, while those in aqueous ammonia are run for 70 ns. The first 5 ns are excluded from the analysis.

2.2.3. Free Energy Calculations. The transferability of the polarizable ion−NH_3 model to bulk solutions is assessed by calculating the intrinsic free energy of solvation of each ion in liquid ammonia at T = 298.15 K and p = 9.9 atm. Two approaches are used for this purpose. In the first, the intrinsic solvation free energies are calculated using free energy perturbation (FEP). Specifically, the solvation free energy is evaluated from the transformation of one alkali ion, M^+, into a "dummy" atom having no charge and no LJ parameters:

$$\Delta G^{\text{intr}}_{\text{solv}} \equiv \Delta G_{\text{solv}}(M^+) - \Delta G_{\text{solv}}(\text{dummy}) = -\Delta G_{\text{mut}}(M^+ \rightarrow \text{dummy}) \quad (3)$$

where ΔG_{mut} is the relative free energy for the alchemical $M^+ \rightarrow$ dummy "mutation" and $\Delta G_{\text{solv}}(\text{dummy}) = 0$. The transformation in performed in 21 steps, controlled by a scaling parameter λ which takes the following values: 0, 0.00001, 0.0001, 0.001, 0.01, 0.05, 0.1, 0.2, 0.3, 0.4, 0.5, 0.6, 0.7, 0.8, 0.9, 0.95, 0.99, 0.999, 0.9999, 0.99999, and 1.[44] Each λ window is equilibrated for 150 ps, followed by subsequent data collection for 350 ps. Each mutation is performed in the forward and backward directions in three independent replicates, in order to confirm the convergence and estimate the error on the calculated values.

In the second approach, the solvation free energy is decomposed into three contributions calculated following a free energy perturbation protocol established previously[39,53,54]

$$\Delta G^{\text{intr}}_{\text{solv}} = \Delta G_{\text{elec}} + \Delta G_{\text{disp}} + \Delta G_{\text{rep}} \quad (4)$$

where ΔG_{elec} is the electrostatic component of the solvation free energy and ΔG_{disp} and ΔG_{rep} are respectively the attractive (dispersive) and repulsive components of the LJ interaction. Each of the three components is calculated from independent simulations. The electrostatic and dispersive components are computed using thermodynamic integration, with the λ parameter taking the values 0, 0.1, 0.2, 0.3, 0.4, 0.5, 0.6, 0.7, 0.8, 0.9, and 1. The repulsive term is computed using a soft-core scheme[53] and unbiased using the weighted histogram analysis method (WHAM).[55] Values of λ = 0, 0.05, 0.1, 0.15, 0.2, 0.25, 0.3, 0.35, 0.4, 0.5, 0.6, 0.7, 0.8, 0.9, and 1 are used to calculate ΔG_{rep}.[39] Solvation free energies calculated from both approaches are within statistical error. On the basis of multiple runs, the error on the calculated values is ±0.2 kcal/mol.

2.2.4. Potential of Mean Force Calculations. Potentials of mean force (PMFs) between each ion (Li^+, Na^+, K^+, Rb^+, or Cs^+) and one ammonia molecule in pure water and between each ion and one water molecule in pure ammonia are calculated using umbrella sampling, according to a previously reported procedure.[47] For these simulations, each system is composed of one alkali ion and one ligand (ammonia or water) solvated in 249 solvent molecules (water for the ammonia ligand and ammonia for the water ligand). The distance between the ion and the heavy atom of the ligand (N for ammonia or O for water) is used as a reaction coordinate and is sampled from 1 to 10 Å using 0.5-Å separated windows. A harmonic potential of force constant 10 kcal/mol/Å^2 is applied to bias the sampling. Each window is simulated for 2.3 ns, and the last 2 ns are used to construct the unbiased PMF using WHAM.[56] To facilitate comparison, all PMFs are evaluated at the normal boiling point of ammonia (239.8 K and 1 atm).

3. RESULTS AND DISCUSSION

3.1. Ab Initio Optimized Structures. High-level ab initio calculations of small alkali ion−ammonia (binary) and alkali ion−ammonia−water (ternary) clusters can help in understanding the onset of bulk solvation as the size of the cluster increases. Only a limited number of ab initio studies have been published on alkali ion−ammonia clusters larger than the dimer,[18,19,21,24,27,28] and to the best of our knowledge no ab initio investigations have been reported on alkali ion−ammonia−water ternary clusters to date.

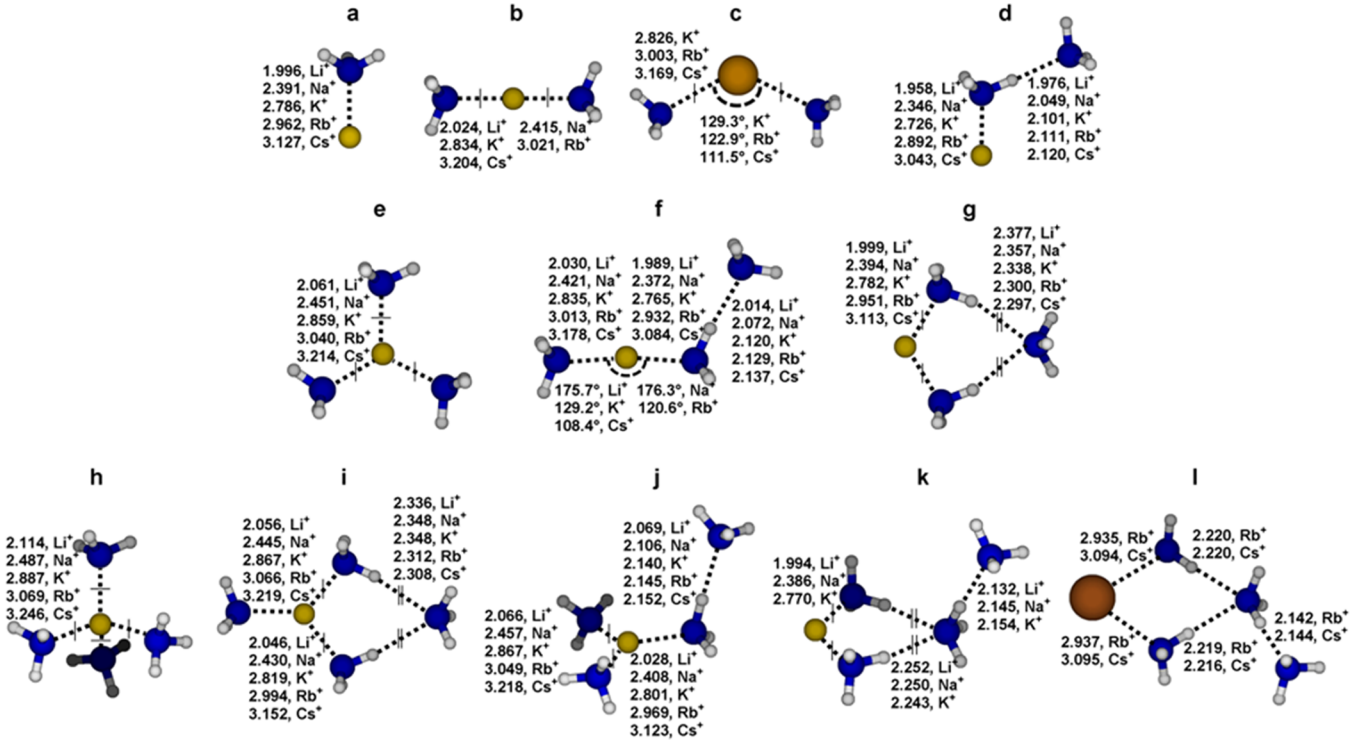

Figure 1. Optimized structures of alkali ion−ammonia clusters $M^+(NH_3)_n$ (M^+ = Li^+, Na^+, K^+, Rb^+, Cs^+ and n = 1−4) at the MP2 level (see the Methods section for details). Selected geometrical parameters ($M^+\cdots N$ and $H\cdots N$ distances in Å and $N\cdots M^+\cdots N$ angles in degrees) are reported. Equal atom−atom distances are indicated with single or double dashes. The structures are illustrated with Li^+ complexes, except for panels *c* (illustrated with K^+) and *l* (illustrated with Rb^+). Corresponding parameters for other alkali ions are reported.

Since the purpose of studying the binary and ternary complexes is simply to validate the optimized potential model, not all stable conformers will be reported for all systems.

3.1.1. $M^+(NH_3)_n$ Clusters. While previous ab initio investigations considered mainly the global energy minima,[19,21,27,28] in this study local energy minima of $M^+(NH_3)_n$ clusters (n = 1−4) are considered as well. Figure 1 shows the various optimized geometries and some of their characteristic parameters, and Table 1 lists binding energies with (E^{CP}) and without (E) correction for BSSE, in addition to binding energies calculated with the optimized Drude model (E^{MM}, see section 3.3). The distance between the alkali cation and directly coordinated ammonia molecules increases on going from Li^+ to Cs^+, due to increasing ion size (see Figure 1). The distance also increases with the number of ammonia molecules in the ion's first coordination shell (see Figure 1a,b,e,h).

Optimization of M^+−NH_3 dimers shows stable structures with C_{3v} symmetry. The optimized structures of alkali ions Li^+, Na^+, and K^+ show uncorrected binding energies E = −40.85, −28.22, and −20.71 kcal/mol, respectively. In comparison, Kerdcharoen and Hannongbua[19] reported values E = −45.5, −33.1, and −21.2 kcal/mol, respectively, at the MP2/6-31G(d,p) level of theory. The BSSE-corrected values E^{CP} = −38.71, −26.43, and −19.56 kcal/mol are in good agreement with the experimental binding enthalpies at room temperature (ΔH_{298}) of −39.1,[57] −25.4 ± 1.3,[58] and −18.9 ± 1.7 kcal/mol[59] reported for NH_3 in complex with Li^+, Na^+, and K^+, respectively. Full-electron calculations on dimers of Li^+, Na^+, and K^+ with ammonia yield E^{CP} = −38.98, −26.73, and −19.58 kcal/mol, respectively, in very close agreement with the FC calculations. The calculated binding energies of Rb^+ and Cs^+ complexes with NH_3 (E^{CP} = −16.69 and −14.94 kcal, respectively) are in good agreement with the dissociation energies of −16.2 and −14.2 kcal/mol calculated by Lim et al. at the CCSD(T) level of theory.[26]

Alkali ions are reported to bind water less strongly than ammonia.[23,57,58] For the purpose of comparison, the interaction energies of Li^+, Na^+, K^+, Rb^+, and Cs^+ with water are calculated at the same level of theory. We find E^{CP} = −33.40, −23.09, −17.88, −15.24, and −13.73 kcal/mol, respectively, weaker than the corresponding ion−ammonia binding energies (see Table 1). The optimized ion−water dimers also show $M^+\cdots O$ distances of 1.866 Å for Li^+, 2.266 Å for Na^+, 2.631 Å for K^+, 2.794 Å for Rb^+, and 2.960 Å for Cs^+, shorter than the corresponding $M^+\cdots N$ distances (see Figure 1). The calculated ion−water binding energies are in good agreement with the experimentally reported[60] binding enthalpies ΔH_{298} = −34.0, −24.0, −17.9, −15.9, and −13.7 kcal/mol. This agreement further supports the choice of basis sets employed in this study.

Li^+ and Na^+ show only two stable conformers for the $M^+(NH_3)_2$ cluster (Figure 1b and d), but K^+, Rb^+, and Cs^+ stabilize an additional "bent" isomer (Figure 1c). Conformer **1b** possesses D_{3d} symmetry, with the two NH_3 molecules in staggered orientation, and is the global minimum conformer for both Li^+ and Na^+, in accord with previous ab initio results.[21,24] A previously reported linear structure in which the two ammonia molecules are in eclipsed orientation[28] (D_3 symmetry, not shown in Figure 1) corresponds to a transition state. Conformer **1c** is a bent, C_s-symmetric structure and represents the global minimum energy for K^+, Rb^+, and Cs^+ (see Table 1). Conformer **1d**, with only one ammonia molecule coordinating the ion, is the least stable of the three structures. The E^{CP} value for the ground-state $Li^+(NH_3)_2$ conformer (**1b**), −71.23 kcal/mol, is in agreement

dx.doi.org/10.1021/ct4001069 | J. Chem. Theory Comput. 2013, 9, 2324−2338

Table 1. Binding Energies without and with Correction for BSSE (E and E^{CP}, Respectively) and the Corresponding Binding Energy Calculated Using the Optimized Drude Model (E^{MM}) for the Alkali Ion-Ammonia Clusters $[M^+(NH_3)_n; M^+ = Li^+, Na^+, K^+, Rb^+, Cs^+$ and $n = 1-4]$[a]

	Li^+			Na^+			K^+			Rb^+			Cs^+		
complex (n) [structure][b]	E	E^{CP}	E^{MM}	E	E^{CP}	E^{MM}	E	E^{CP}	E^{MM}	E	E^{CP}	E^{MM}	E	E^{CP}	E^{MM}
1a (1) [1 + 0]	−40.85	−38.71	−38.74	−28.22	−26.43	−26.43	−20.71	−19.56	−19.59	−17.10	−16.69	−16.89	−15.55	−14.94	−15.07
1b (2) [2 + 0]	−76.08	−71.23	−69.94	−53.45	−49.55	−49.19	−38.60	−36.46	−36.42	−31.87	−31.16	−31.44	−28.67	−27.62	−27.87
1c (2) [2 + 0]	–	–	–	–	–	–	−38.73	−36.53	−36.43	−32.03	−31.27	−31.55	−29.10	−27.95	−28.14
1d (2) [1 + 1]	−55.59	−51.72	−51.98	−40.65	−37.27	−37.21	−31.68	−28.91	−29.08	−26.83	−25.76	−25.82	−25.00	−23.70	−23.62
1e (3) [3 + 0]	−101.88	−94.58	−91.22	−73.49	−67.90	−67.14	−54.47	−51.17	−50.89	−45.15	−44.06	−44.32	−40.94	−39.32	−39.63
1f (3) [2 + 1]	−89.13	−82.59	−81.26	−64.84	−59.37	−58.92	−48.86	−45.09	−45.13	−41.05	−39.65	−39.78	−37.87	−36.06	−36.10
1g (3) [2 + 1]	−86.38	−80.56	−77.20	−62.88	−57.86	−57.20	−48.96	−44.84	−44.86	−41.72	−40.03	−39.94	−38.80	−36.69	−36.60
1h (4) [4 + 0]	−120.35	−110.38	−106.06	−89.68	−82.07	−81.26	−67.89	−63.37	−62.96	−56.46	−55.05	−55.30	−51.38	−49.31	−49.64
1i (4) [3 + 1]	−113.25	−104.40	−100.09	−83.77	−76.60	−75.58	−64.11	−58.99	−58.81	−54.21	−52.26	−52.23	−50.10	−47.52	−47.58
1j (4) [3 + 1]	−113.18	−104.24	−100.81	−83.73	−76.58	−75.79	−63.78	−58.96	−58.96	−53.46	−51.76	−51.89	−49.11	−46.81	−46.97
1k (4) [2 + 1 + 1]	−95.96	−88.37	−84.60	−71.93	−65.17	−64.20	−57.60	−51.71	−51.78	–	–	–	–	–	–
1l (4) [2 + 1 + 1]	–	–	–	–	–	–	–	–	–	−49.67	−47.24	−47.55	−46.63	−43.77	−44.05

[a] All energies are in kcal/mol. [b] Total number of ammonia molecules in parentheses. In square brackets are the numbers of ammonia molecules in the ion's first, second, and third (if any) coordination shells (see Figure 1). The dashes indicate that the conformation is unstable.

with MP2(full)/6-311+G(d,p) results from the literature (E^{CP} = −71.23 kcal/mol).[21]

Three conformers are identified for the $M^+(NH_3)_3$ tetramer (see Figure 1e,f,g). Isomer **1e** possesses C_{3h} symmetry and is the global energy minimum. The E^{CP} value for the $Li^+(NH_3)_3$ global minimum is −94.58 kcal/mol, compared to −92.06 kcal/mol calculated at the MP2(full)/6-311+G(d,p) level of theory.[21] Both isomers **1f** and **1g** have C_s symmetry, and only two NH_3 molecules are directly coordinating the metal ion. Structure **1f** is more stable than structure **1g** for Li^+, Na^+, and K^+, but less stable for Rb^+ and Cs^+ (see Table 1).

Four conformers are located for the $M^+(NH_3)_4$ pentamer (see Figure 1h–l). In the global minimum structure (**1h**), the four ammonia molecules coordinate the ion in a T_d symmetry. Structures **1i** and **1j**, with the ion coordinated by only three ammonia molecules, have comparable stabilities (see Table 1). For these structures, the coordination geometry is determined by the size of the ion: trigonal quasi-planar for Li^+ and Na^+ (as depicted in Figure 1i) but trigonal pyramidal for the larger ions (with the ammonia molecule not involved in a hydrogen bond bent out of the trigonal plane; structure not shown). For conformer **1j**, the coordination is trigonal quasi-planar for Li^+, Na^+, and K^+ but trigonal pyramidal for Rb^+ and Cs^+ (with the ion displaced toward the second-shell ammonia molecule; structure not shown). In the least stable conformer (**1k** for Li^+, Na^+, and K^+ and **1l** for Rb^+ and Cs^+), only two ammonia molecules are bonded to the cation.

As shown in Figure 1d,f,j, the distance between hydrogen-bonded ammonia molecules, represented by the H···N distance, increases on going from Li^+ to Cs^+ yet is always shorter than in the isolated ammonia dimer (which has an H···N distance of 2.263 Å at the MP2(FC)/6-311++G(d,p) level). Comparison between structures **1a** and **1d**, between structures **1b**/**1c** and **1f**, and between structures **1e** and **1j** shows that the presence of a second-shell ammonia molecule reduces the M^+···N distance between the ion and its coordinating ammonia molecules. The shortening of N···N and M^+···N distances in "M^+···N–H···N" motifs indicates binding cooperativity: The ion and second-shell ammonia enhance the polarity of the first-shell ammonia molecule, which strengthens both ion–ammonia and ammonia–ammonia interactions. On the other hand, comparison between structures **1a**, **1b**/**1c**, **1e**, and **1h** shows that adding ammonia molecules to the ion's first shell increases the M^+···N distance. While steric factors might contribute to the elongation of M^+···N bonds in larger clusters, in smaller clusters the elongation is mostly due to the "N···M^+···N" motif creating binding anticooperativity: The ion induces opposite dipoles in the ammonia molecules, which creates a repulsive electrostatic force between them.[47,48]

To analyze the binding cooperativity or anticooperativity between ion–ammonia and ammonia–ammonia interactions, we calculate the E^{coop} parameter for complexes **1b** and **1d**, in accord with a previous approach:[47,48]

$$E^{coop} = E^{tot} - E^{1}_{M^+-NH_3} - E^{2}_{M^+-NH_3} - E_{NH_3-NH_3} \quad (5)$$

where E^{tot} is the total binding energy of the trimer, $E^{1}_{M^+-NH_3}$ and $E^{2}_{M^+-NH_3}$ are the binding energies between the ion and each of the ammonia molecules (labeled 1 and 2), and $E_{NH_3-NH_3}$ is the binding energy between the two ammonia molecules. All energy terms are calculated in the geometry found in the optimized trimers (see Figure 1b and d). Binding energies of the ammonia dimers, $E_{NH_3-NH_3}$, are calculated at the MP2(FC)/6-311++G(d,p)

Table 2. BSSE-Corrected Complexation Energies Calculated at the MP2 Level and Corresponding Interaction Energies Calculated Using the Optimized Drude Model (In Parentheses)[a]

	complex **1b**					complex **1d**				
energy[b]	Li^+	Na^+	K^+	Rb^+	Cs^+	Li^+	Na^+	K^+	Rb^+	Cs^+
E^{tot}	−71.23 (−69.94)	−49.55 (−49.19)	−36.46 (−36.42)	−31.16 (−31.55)	−27.62 (−28.18)	−51.72 (−51.98)	−37.27 (−37.21)	−28.91 (−29.08)	−25.76 (−25.82)	−23.70 (−23.62)
$E^1_{M^+-NH_3}$	−38.68 (−39.11)	−26.44 (−26.82)	−19.58 (−19.87)	−16.65 (−17.15)	−14.91 (−15.30)	−38.59 (−39.86)	−26.24 (−27.22)	−19.26 (−20.17)	−16.42 (−17.38)	−14.60 (−15.49)
$E^2_{M^+-NH_3}$	−38.68 (−39.11)	−26.44 (−26.82)	−19.58 (−19.87)	−16.65 (−17.15)	−14.91 (−15.30)	−9.80 (−6.41)	−7.99 (−5.65)	−6.81 (−5.08)	−6.06 (−4.79)	−5.78 (−4.56)
$E_{NH_3-NH_3}$	2.73 (1.52)	1.54 (0.99)	0.93 (0.68)	0.60 (0.71)	0.49 (0.71)	−1.03 (−1.82)	−1.51 (−2.27)	−1.75 (−2.40)	−2.08 (−2.43)	−2.10 (−2.45)
E^{coop}	3.41 (6.76)	1.79 (3.46)	1.77 (2.64)	1.55 (2.04)	1.72 (1.71)	−2.30 (−3.89)	−1.53 (−2.07)	−1.08 (−1.43)	−1.20 (−1.22)	−1.22 (−1.12)

[a]All energies are in kcal/mol. [b]E^{tot} is the total binding energy, $E^1_{M^+-NH_3}$ and $E^2_{M^+-NH_3}$ are the binding energies between the metal ion and each ammonia molecule, and $E_{NH_3-NH_3}$ is the interaction energy between the two ammonia molecules. While E^{tot} is obtained from relaxed trimer geometries (with NH bonds constrained with the SHAKE algorithm in Drude model calculations), the other three terms are calculated using coordinates extracted from the trimer geometries. $E_{NH_3-NH_3}$ is calculated at the MP2(FC)/6-311++G(d,p) level for complexes of Li^+, Na^+, and K^+ and at the MP2(full)/6-311+G(3df,2p) level for complexes of Rb^+ and Cs^+. E^{coop} is the energy due to cooperativity or anticooperativity between molecular interactions, calculated according to eq 5.

level for trimer complexes of Li^+, Na^+, and K^+ and at the MP2(full)/6-311+G(3df,2p) level for Rb^+ and Cs^+ trimers. The calculated data, together with those from the Drude model, are reported in Table 2.

According to eq 5, a negative E^{coop} indicates that the total interaction energy is greater (more negative) than the sum of the pairwise interactions, showing cooperativity between the individual interactions. On the other hand, a positive E^{coop} indicates binding anticooperativity. Table 2 shows cooperativity between ion−ammonia and ammonia−ammonia interactions for complex **1d** and anticooperativity between the two ion−ammonia interactions in complex **1b**. The shortening of $M^+\cdots N$ distances in complexes **1b** and **1e** when a second-shell ammonia molecule is added (see Figure 1f and j) is similarly reflecting cooperativity between the individual interactions.

To understand the origin of preferential solvation, it is instructive to compare the energies of Table 1 with those of analogous ion−water clusters. Glendening and Feller[61] have reported CP-corrected binding energies for alkali ion hydrates, $M^+(H_2O)_n$ (n = 1−6), calculated at the MP2/6-31+G*//RHF/6-31+G* level, with effective core potentials for Rb^+ and Cs^+. For Li^+, they find E^{CP} = −34.5 kcal/mol for the monohydrate (n = 1), −64.4 kcal/mol for the dihydrate (n = 2), −87.5 kcal/mol for n = 3, and −104.1 kcal/mol for n = 4.[61] While these binding energies are weaker than those for ammonia complexes (see Table 1), they fall less rapidly as the lithium ion's first solvation shell gets populated. Each additional ammonia molecule (going from n = 1 to 4) increases the complexation energy of the cluster by −38.71, −32.52, −23.35, and −15.80 kcal/mol (see Table 1), while each water molecule increases the energy by −34.5, −29.9, −23.1, and −16.6 kcal/mol.[61] The reversal in the relative ammonia/water affinity between tri- and tetracoordinated Li^+ ions is due to the larger size of ammonia molecules, which creates greater steric hindrance at high coordination numbers. A similar trend is observed for the other alkali metal ions. For instance, binding of the first water molecule results in E^{CP} = −24.3 kcal/mol for Na^+, −18.9 kcal/mol for K^+, −16.1 kcal/mol for Rb^+, and −14.1 kcal/mol for Cs^+,[61] which is systematically weaker than the corresponding ion−ammonia energies (see Table 1), but binding of the fourth water molecule (from "[3 + 0]" to "[4 + 0]" ion−water clusters) increases E^{CP} by −14.0 kcal/mol for Na^+, −12.8 kcal/mol for K^+, −11.4 kcal/mol for Rb^+, and −14.8 kcal/mol for Cs^+,[61] which is comparable or *stronger* than the corresponding increases in E^{CP} from "[3 + 0]" to "[4 + 0]" ion−ammonia clusters (Figure 1e and h): −14.17 kcal/mol for Na^+, −12.20 kcal/mol for K^+, −10.99 kcal/mol for Rb^+, and −9.99 kcal/mol for Cs^+ (see Table 1).

3.1.2. $M^+(NH_3)_n(H_2O)_m$ Clusters. The optimized structures of ternary $M^+(NH_3)_n(H_2O)_m$ clusters (n, m = 1−3 and $n + m \leq 4$) are presented in Figure 2. Table 3 shows the ab initio binding energies of the structures, together with binding energies calculated with the optimized Drude model. All stable conformers are identified for the trimer and tetramer Li^+ clusters (Figure 2a−h), but for the sake of comparison only structurally similar isomers are considered for other alkali ions. For the "$n + m$ = 4" mixed clusters, only isomers derived from the tetrahedral arrangement of four molecules around the ion are considered.

Two stable isomers are presented for the $M^+(NH_3)(H_2O)$ trimer (Figure 2a and b). Structure **2a** is quasi-linear for Li^+ and Na^+ but bent for the other alkali ions. The global minimum is structure **2a** for Li^+, Na^+, and K^+ and structure **2b** for Rb^+ and

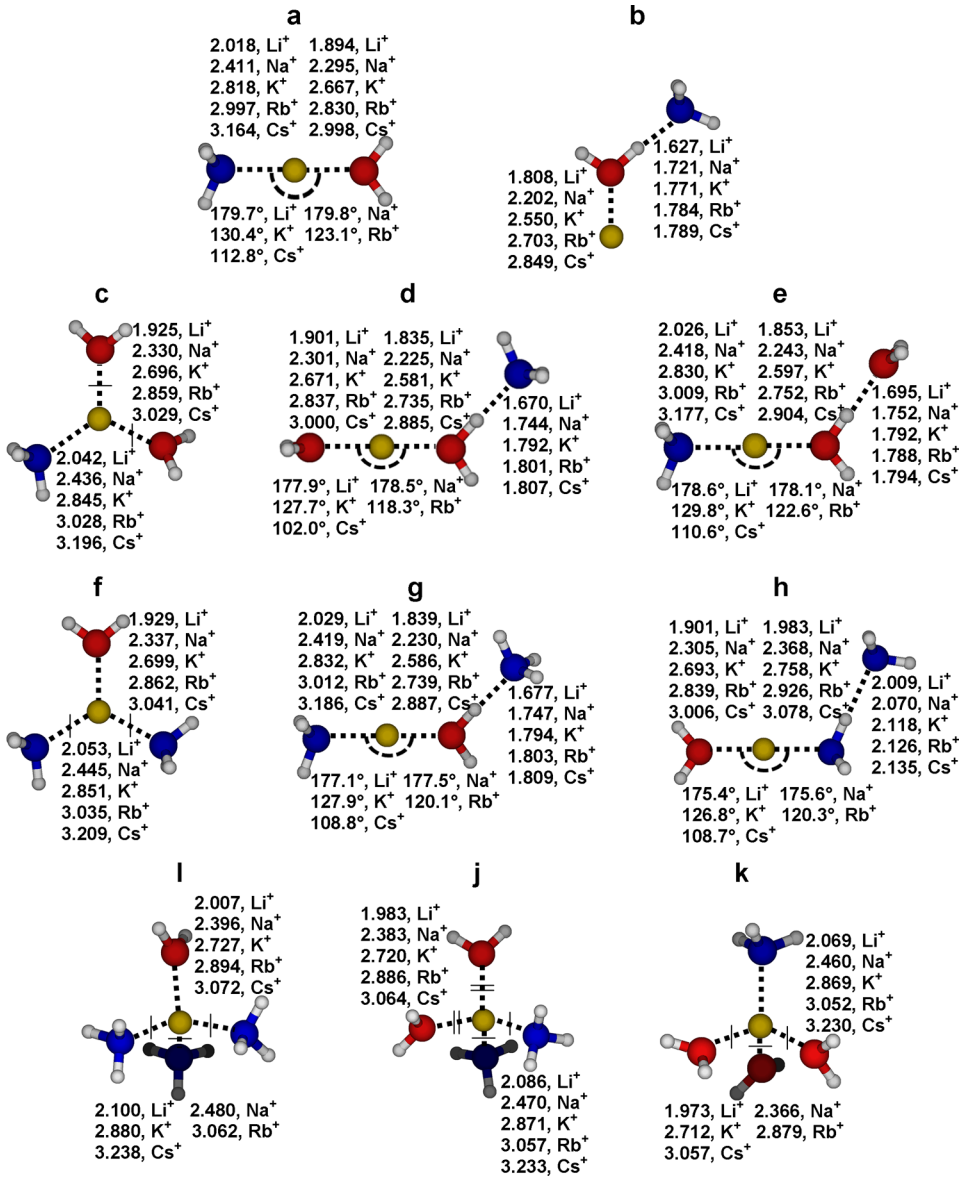

Figure 2. Optimized structures of the alkali ion–ammonia–water ternary clusters $M^+(NH_3)_n(H_2O)_m$ ($M^+ = Li^+$, Na^+, K^+, Rb^+, Cs^+, with n, $m = 1–3$ and $n + m \leq 4$) at the MP2 level (see the Methods section for details). Selected geometrical parameters are reported ($M^+\cdots N$, $M^+\cdots O$, $H\cdots N$, and $H\cdots O$ distances in Å and $N\cdots M^+\cdots O$ and $O\cdots M^+\cdots O$ angles in degrees). Equal atom–atom distances are crossed with single or double bars. The structures are illustrated with Li^+ complexes, but corresponding parameters for other alkali ion complexes are reported.

Cs^+ (see Table 3). Optimization of the structure in which H_2O is in the second coordination shell of the ion did not show a stable conformer, likely due to N–H···O hydrogen bonds being weaker than O–H···N bonds.[44] The dicoordinated trimers of Li^+, Na^+, K^+, Rb^+, and Cs^+ (Figure 2a) are respectively 4.49, 2.87, 1.36, 1.16, and 0.95 kcal/mol less stable than the equivalent complexes of one ion and two ammonia molecules (Figure 1b and c). On the other hand, the trimers of Figure 2b are respectively 4.20, 3.59, 4.32, 4.59, and 4.67 kcal/mol *more* stable than the corresponding ammonia-only complexes (Figure 1d).

Three stable conformations of the $M^+(NH_3)(H_2O)_2$ tetramer are shown in Figures 2c–e. The structures have quasi-planar geometries, except for the K^+, Rb^+, and Cs^+ complexes of structure **2d**, for which the $O\cdots M^+\cdots O\cdots N$ dihedral angle significantly deviates from zero. The stability of the complexes follows the order **2c** > **2d** > **2e** for Li^+, Na^+ and K^+; **2d** > **2c** > **2e** for Rb^+; and **2d** > **2c** ≈ **2e** for Cs^+ (see Table 3).

Equivalent stable conformations for the $M^+(NH_3)_2(H_2O)$ tetramer are shown in Figure 2f–h. Comparison of the binding energies of tricoordinated structures **1e**, **2f**, and **2c** (see Tables 1 and 3) shows a decrease in stability as first-shell ammonia molecules are replaced with water (**1e** > **2f** > **2c**). Ammonia is more stable than water in the first solvation shell of the ion if it is not involved in a hydrogen bond with a second-shell molecule (**2g** > **2d**) but is *less* stable than water if it is (**2h** < **2d**). Comparison between binding energies reported for structures **2g** and **2e** shows that water in the ion's first solvation shell is preferably bound to ammonia from the second solvation shell, due to O–H···N hydrogen bonds being slightly stronger than O–H···O bonds.[44]

The clusters obtained by substituting ammonia molecules with water in the tetrahedral $M^+(NH_3)_4$ pentamer are reported in Figure 2i–k. Similarly to what is observed for the tetramer (**1e** > **2f** > **2c**), the stability of the tetrahedral pentamer

dx.doi.org/10.1021/ct4001069 | J. Chem. Theory Comput. 2013, 9, 2324–2338

Table 3. Binding Energies with and without Correction for BSSE (E and E^{CP}, Respectively) and the Corresponding Binding Energy Calculated Using the Optimized Drude Model (E^{MM}) for the Alkali Ion−Ammonia−Water Ternary Clusters $[M^+(NH_3)_n(H_2O)_m$, M^+ = Li^+, Na^+, K^+, Rb^+, Cs^+, with n, m = 1−3 and $n + m \leq 4]^a$

	Li^+			Na^+			K^+			Rb^+			Cs^+		
complex	E	E^{CP}	E^{MM}	E	E^{CP}	E^{MM}	E	E^{CP}	E^{MM}	E	E^{CP}	E^{MM}	E	E^{CP}	E^{MM}
2a	−71.64	−66.74	−68.09	−50.36	−46.68	−47.86	−37.35	−35.17	−35.20	−30.91	−30.11	−30.86	−28.14	−27.00	−27.03
2b	−60.69	−55.92	−56.22	−44.79	−40.80	−41.52	−36.68	−33.23	−32.62	−31.95	−30.35	−29.85	−30.20	−28.37	−26.70
2c	−95.49	−88.14	−89.50	−68.66	−63.45	−65.55	−52.28	−49.02	−49.10	−43.37	−42.19	−43.44	−39.46	−37.78	−37.87
2d	−89.47	−82.05	−84.18	−65.99	−60.12	−62.12	−52.50	−48.11	−47.73	−45.05	−43.09	−43.34	−42.08	−39.74	−38.34
2e	−88.56	−81.36	−82.59	−65.26	−59.39	−60.79	−50.82	−46.59	−46.83	−43.24	−41.35	−42.06	−40.18	−37.90	−37.69
2f	−98.74	−91.54	−90.35	−71.10	−65.74	−66.35	−53.39	−50.07	−50.02	−44.27	−43.14	−43.89	−40.21	−38.58	−38.76
2g	−93.59	−86.11	−85.73	−68.91	−62.86	−63.29	−53.77	−49.36	−48.86	−46.10	−44.18	−43.93	−42.97	−40.63	−39.40
2h	−84.90	−78.30	−79.66	−61.86	−56.61	−57.72	−47.58	−43.87	−44.01	−40.02	−38.59	−39.20	−37.00	−35.18	−35.07
2i	−118.06	−107.94	−105.69	−87.78	−80.41	−80.83	−67.04	−62.55	−62.38	−55.80	−54.32	−55.08	−50.81	−48.69	−49.00
2j	−116.07	−105.77	−105.49	−86.05	−78.61	−80.48	−66.49	−61.38	−61.82	−55.14	−53.60	−54.88	−50.24	−48.08	−48.36
2k	−114.32	−103.57	−105.50	−84.27	−77.01	−80.22	−65.48	−60.93	−61.28	−54.49	−52.89	−54.69	−49.67	−47.48	−47.70

[a] All energies are in kcal/mol.

decreases as NH_3 molecules are replaced by water (**1h** > **2i** > **2j** > **2k**; see Tables 1 and 3).

In summary, alkali metal ions are preferentially coordinated by ammonia relative to water at least up to tetra-coordinated structures. Higher coordination numbers might however favor H_2O over NH_3, due to steric effects. The ammonia preference is partially reversed when molecules are added to the ion's second solvation shell. While an NH_3 molecule in the first solvation shell will form weak N−H···N or N−H···O hydrogen bonds with NH_3 or H_2O molecules in the second solvation shell, a first-shell H_2O molecule will form strong O−H···N or O−H···O hydrogen bonds. The presence of a second shell therefore enhances the stability of H_2O in the first solvation shell relative to NH_3.

Comparison between the M^+···N, M^+···O, and N···H(H_2O) distances in the ion−ammonia, ion−water (see section 3.1.1), and ammonia−water (1.974 Å at the MP2(FC)/6-311++G(d,p) level) dimers, and the corresponding distances in complexes **2a** and **2b**, signals cooperativity between ion−water and ammonia−water interactions in complex **2b** ($E^{coop} < 0$) and anticooperativity between ion−ammonia and ion−water interactions in complex **2a** ($E^{coop} > 0$). The E^{coop} parameter in the two complexes is again calculated as the difference between the total interaction energy and the sum of the different pairwise interactions:

$$E^{coop} = E^{tot} - E_{M^+-H_2O} - E_{M^+-NH_3} - E_{H_2O-NH_3} \quad (6)$$

Table 4 shows positive E^{coop} for complexes **2a** and negative E^{coop} for complexes **2b**. Similarly, comparing the structural parameters of complex **2a** with those of complexes **2e**, **2g**, and **2h** shows cooperativity between first and second shell interactions.

3.2. Ab Initio Potential Energy Curves. Figure 3 shows ab initio potential energy surfaces together with the corresponding surfaces calculated with the optimized Drude model (see section 3.3). These curves are calculated by scanning the M^+···N distance and the M^+···H−N angle in the $M^+(NH_3)$ dimers, while keeping the NH_3 geometry fixed. Curve a represents the binding energy as a function of the distance between the ion and NH_3 in their C_{3v}-symmetric orientation. Curve b shows that the binding energy decreases as the M^+···H−N angle deviates from the equilibrium value, ∼116°. These two curves are used to optimize the Drude model for the ion−ammonia interactions.

3.3. Optimized Drude Model. The optimized pair-specific LJ parameters of the polarizable potential model for alkali ion−ammonia interactions are reported in Table 5. As shown in Figure 3, the Drude-model PESs are in good agreement with ab initio results. The narrow shape of the Drude-model distance PESs (Figure 3a) is likely due to the steepness of the Lennard-Jones $1/r^{12}$ repulsive potential.[62] Although "softer" functional forms have been proposed,[63] we use the $1/r^{12}$ form to retain compatibility with the other components of the Drude polarizable force field and with standard nonpolarizable force fields.

Table 1 shows that the Drude model gives binding energies of ion−ammonia binary clusters in good agreement with ab initio calculations: For all Li^+, Na^+, K^+, Rb^+, and Cs^+ clusters (Figure 1), maximum errors of respectively 4.3, 1.5, 0.6, 1.2, and 0.9% and average unsigned errors of respectively 2.7, 0.9, 0.3, 0.5, and 0.5% are found. For ion−ammonia dimers, the model yields M^+···N separations of 2.105 Å for Li^+, 2.456 Å for Na^+, 2.788 Å for K^+, 2.972 Å for Rb^+, and 3.129 Å for Cs^+, in good agreement with MP2 results (see Figure 1a). It also captures the geometric variations of clusters as ammonia molecules are added.

Table 4. BSSE-Corrected Complexation Energies Calculated at the MP2 Level and Corresponding Interaction Energies Calculated Using the Optimized Drude Model (In Parentheses)[a]

	complex **2a**					complex **2b**				
energy[b]	Li^+	Na^+	K^+	Rb^+	Cs^+	Li^+	Na^+	K^+	Rb^+	Cs^+
E^{tot}	−66.74 (−68.09)	−46.68 (−47.86)	−35.17 (−35.20)	−30.12 (−30.86)	−27.00 (−26.70)	−55.92 (−56.22)	−40.80 (−41.52)	−33.23 (−32.62)	−30.35 (−29.85)	−28.37 (−27.03)
$E_{M^+-H_2O}$	−33.39 (−35.74)	−23.11 (−24.59)	−17.91 (−17.86)	−15.25 (−15.84)	−13.74 (−13.54)	−33.35 (−35.55)	−22.93 (−24.45)	−17.94 (−17.73)	−15.04 (−15.70)	−13.43 (−13.37)
$E_{M^+-NH_3}$	−38.69 (−39.19)	−26.44 (−26.85)	−19.57 (−19.91)	−16.67 (− 17.17)	−14.94 (−15.34)	−10.56 (−8.90)	−8.25 (−7.65)	−6.86 (−6.51)	−5.91 (−6.07)	−5.55 (−5.54)
$E_{H_2O-NH_3}$	2.31 (1.38)	1.35 (0.91)	1.04 (0.70)	0.71 (0.66)	0.67 (0.64)	−3.81 (−3.84)	−4.52 (−4.70)	−4.84 (−5.04)	−5.46 (−5.13)	−5.49 (−5.22)
E^{coop}	3.03 (5.46)	1.52 (2.67)	1.27 (1.87)	1.09 (1.49)	1.01 (1.54)	−8.20 (−7.93)	−5.10 (−4.72)	−3.59 (−3.34)	−3.94 (−2.95)	−3.90 (−2.90)

[a]All energies are in kcal/mol. [b]E^{tot} is the total binding energy, $E_{M^+-H_2O}$ and $E_{M^+-NH_3}$ are the binding energies between the metal ion and the individual molecules, and $E_{H_2O-NH_3}$ is the interaction energy between water and ammonia. While E^{tot} is obtained from relaxed trimer geometries (with NH bonds constrained with the SHAKE algorithm in Drude model calculations), the other three terms are calculated using coordinates extracted from the trimer geometries. $E_{H_2O-NH_3}$ is calculated at the MP2(FC)/6-311++G(d,p) level for complexes of Li^+, Na^+, and K^+ and at the MP2(full)/6-311+G(3df,2p) level for complexes of Rb^+ and Cs^+. E^{coop} is the energy due to cooperativity between molecular interactions, calculated according to eq 6.

For instance, the $Li^+\cdots N$ distance increases with the metal coordination number from 2.105 Å for the dimer (Figure 1a) to 2.148 Å for the trimer (Figure 1b), 2.204 Å for the tetramer (Figure 1e), and 2.260 Å for the pentamer (Figure 1h). For complex **1d**, the Drude model shows a $Li^+\cdots N$ distance of 2.072 Å and a $H\cdots N$ distance of 2.167 Å, which are respectively 0.033 Å and 0.185 Å shorter than the corresponding distances in the isolated dimers, in line with the ab initio trend. As for the ab initio geometries, hydrogen bonds between first and second-shell ammonia molecules are longer for large ions (Rb^+, Cs^+) than for small ions (Li^+, Na^+) when the second-shell ammonia forms a single hydrogen bond (as in complexes **1d**, **1f**, and **1j**) but are shorter for large ions when it forms two (as in complexes **1g** and **1i**). The Drude model also reproduces the cooperativity and anticooperativity observed in ion−ammonia clusters (see Table 2).

In combination with the SWM4-NDP water model, the Drude model for NH_3 yields binding energies of ion−ammonia−water clusters in good agreement with ab initio MP2 results (see Table 3). For all Li^+, Na^+, K^+, Rb^+, and Cs^+ clusters (Figure 2), maximum errors of 2.6, 4.2, 1.8, 3.4, and 3.5% and average unsigned errors of 1.4, 2.2, 0.6, 1.9, and 1.4% are found. The models reproduce the MP2 relative stabilities of the various structural arrangements of ligands around the metal ion. They also reproduce the cooperative and anticooperative binding observed in the ternary trimers (see Table 4).

The Drude model for alkali ion−water interactions[39] shows binding energies of the ion−water dimer of −35.92, −24.64, −17.90, −15.87, and −13.54 kcal/mol and $M^+\cdots O$ distances of 1.906, 2.242, 2.620, 2.791, and 3.018 Å (going from Li^+ to Cs^+). While the ion−ammonia model is optimized to reproduce MP2 binding energies of M^+-NH_3 dimers, the ion−water model[39] was optimized to reproduce the experimental hydration free energies of the ions. For the Li^+ and Na^+ monohydrates, the Drude model slightly overestimates the MP2-calculated binding energies (by 2.5 kcal/mol for the lithium−water pair and by 1.55 kcal/mol for the sodium−water pair; see section 3.1.1). This is likely the reason why the combined Drude models for NH_3 and H_2O underestimate the increase in stability going from Li^+ or Na^+ ions coordinated by 1 ammonia and 3 water molecules (conformer **2k**) to ions coordinated by four ammonia molecules (conformer **1h**). For Li^+, the complexation energy goes from −103.57 to −110.38 kcal/mol for the MP2 calculations but from −105.50 to −106.06 kcal/mol for the Drude model. For Na^+, the complexation energy goes from −77.01 to −82.07 kcal/mol for the MP2 calculations but from −80.22 to −81.26 kcal/mol for the Drude model (see Tables 1 and 3). Since both the ion−water and ion−ammonia models yield solvation free energies in good agreement with experimental data and produce the expected trend for preferential solvation (see sections 3.4 and 3.6), we expect the solvation structures of ions in bulk solvent—whether pure or mixed—to be relatively unaffected by this discrepancy in the gas phase.

The ability of the polarizable model to describe the E^{coop} parameter (as defined in eqs 5 and 6) represents a qualitative advantage over pairwise-additive force fields, which give E^{coop} = 0 by definition.[47,48] In light of the overall good performance of the models, it should be noted that, while the ion−ammonia model is adjusted to reproduce the properties of the ion−ammonia dimer, the ion−water,[39] ammonia−ammonia,[44] and ammonia−water[44] models have not been further adjusted. This suggests that the models can be reliably used to investigate properties of the ion solvated in liquid and aqueous ammonia solutions.

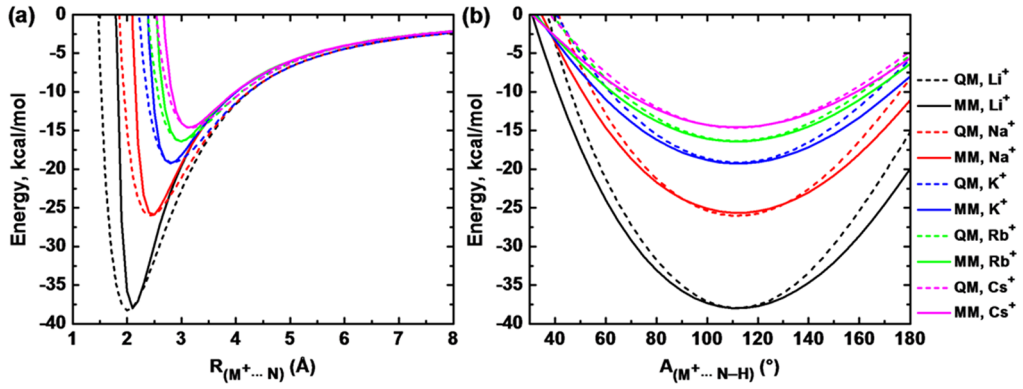

Figure 3. Potential energy curves for $M^+(NH_3)$ (M^+ = Li^+, Na^+, K^+, Rb^+, and Cs^+) from ab initio MP2 calculations (dashed line) and from the polarizable model (solid line). The following coordinates are scanned: (a) $M^+\cdots N$ distance in the direction of ammonia's C_3 axis and (b) $M^+\cdots H-N$ angle at $M^+\cdots N$ distances of 2.1 Å for Li^+, 2.4 Å for Na^+, 2.8 Å for K^+, 3.0 Å for Rb^+, and 3.2 Å for Cs^+.

Table 5. Pair-Specific LJ Parameters for the Interactions of Li^+, Na^+, K^+, Rb^+, and Cs^+ with NH_3

	ion-N LJ parameters[a]		generic LJ parameters[b]	
ion	$E_{min,ion-N}$ (kcal/mol)	$R_{min,ion-N}/2$ (Å)	E_{min} (kcal/mol)	$R_{min}/2$ (Å)
Li^+	0.0156010	1.844186	0.0300000	1.1000000
Na^+	0.0463659	1.888569	0.0315100	1.4616800
K^+	0.0478732	2.082039	0.1419265	1.6866521
Rb^+	0.0487479	2.187484	0.2730669	1.7855083
Cs^+	0.0498201	2.279374	0.2766036	2.0238218

[a]This work. [b]Reproduced from ref 39. Parameters for ion−oxygen and ion−hydrogen interactions are obtained using the Lorentz−Berthelot mixing rules.

3.4. Solvation Free Energy of Alkali Ions in Liquid Ammonia.

To further validate the M^+-NH_3 potential model, we calculate the free energy of solvation of alkali ions in liquid ammonia. The results are reported in Table 6 together with corresponding literature data.[64,65] The data show fair agreement for the solvation free energies of one ion relative to the next in the series. In comparison to liquid ammonia, calculations on alkali ions dissolved in SWM4-NDP water at 298.15 K and 1 atm show intrinsic solvation free energies, ΔG^{intr}_{solv} of −109.8, −85.6, −67.9, −63.0, and −55.8 kcal/mol for Li^+, Na^+, K^+, Rb^+, and Cs^+, respectively.[39] Despite M^+-NH_3 dimers having higher binding energies compared to corresponding M^+-OH_2 dimers, the polarizable model suggests that solvation free energies in water and in ammonia are comparable: $\Delta G^{intr}_{solv,H_2O} - \Delta G^{intr}_{solv,NH_3}$ = −0.3 kcal/mol for Li^+, 0.0 kcal/mol for Na^+, 0.6 kcal/mol for K^+, −1.8 kcal/mol for Rb^+, and −0.4 kcal/mol for Cs^+. This finding—that alkali ions have comparable solvation free energies in water and in ammonia—is supported by experimental results.[64,65] Using thermodynamic data of ions in water and liquid ammonia, Plambeck reported $\Delta G_{solv,H_2O} - \Delta G_{solv,NH_3}$ to be 2.2 kcal/mol for Li^+, −0.4 kcal/mol for Na^+, −1.8 kcal/mol for K^+, −1.0 kcal/mol for Rb^+, and −0.8 kcal/mol for Cs^+.[64] By comparison, using a cluster pair method, Tuttle and co-workers[65] have calculated solvation free energies of Li^+, Na^+, K^+, and Rb^+ in liquid ammonia that are 7.3, 4.3, 2.6, and 2.9 kcal/mol greater

Table 6. Absolute (ΔG^{intr}_{solv}) and Relative ($\Delta\Delta G_{solv}$) Solvation Free Energies of Alkali Ions in Liquid Ammonia,[a] with Corresponding Experimental Values (In Brackets)[b]

ion	ΔG_{elec}	ΔG_{disp}	ΔG_{rep}	ΔG^{intr}_{solv}	$\Delta\Delta G_{solv}$
Li^+	−111.4	−0.2	2.1	−109.5	−23.9 (−28.0[c], −28.2[d])
Na^+	−87.9	−0.6	2.9	−85.6	−17.1 (−19.0[c], −18.8[d])
K^+	−71.4	−1.0	3.9	−68.5	−7.3 (−4.5[c], −5.1[d])
Rb^+	−64.2	−1.4	4.4	−61.2	−5.8 (−5.2[c])
Cs^+	−58.8	−1.7	5.1	−55.4	

[a]$\Delta\Delta G_{solv}$ represents the difference in hydration free energies between consecutive alkali ions. Statistical error on the calculated values is ±0.2 kcal/mol. [b]All values are in kcal/mol. [c]Reference 64. [d]Reference 65.

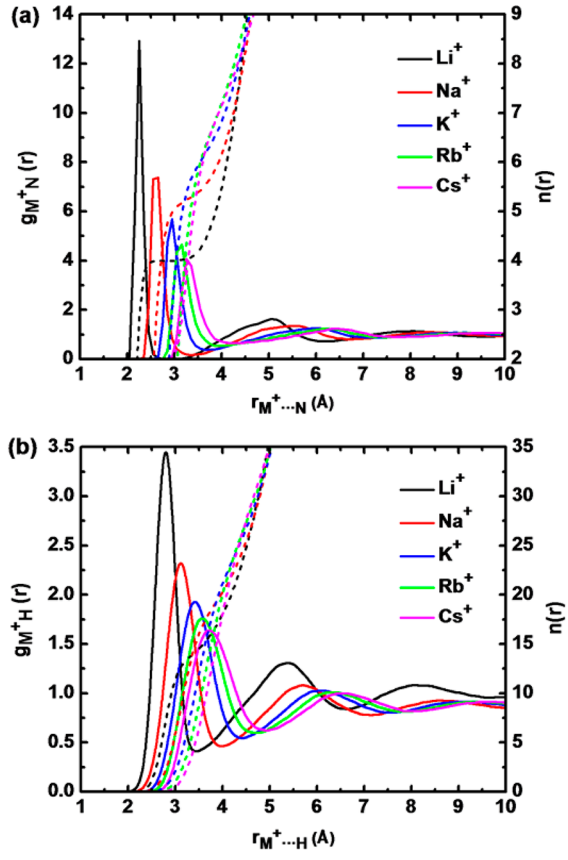

Figure 4. Ion−N (a) and ion−H (b) radial distribution functions (solid curves) and running integration numbers (dashed lines) from molecular dynamics simulations of Li^+ (black), Na^+ (red), K^+ (blue), Rb^+ (green), or Cs^+ (pink) in 250 NH_3 molecules at 239.8 K and 1 atm.

dx.doi.org/10.1021/ct4001069 | J. Chem. Theory Comput. 2013, 9, 2324−2338

Table 7. Characteristic Data of the Radial Distribution Functions, $g_{ion-N}(r)$ and $g_{ion-H}(r)$, for a Single Ion in Liquid Ammonia[a]

	$g_{ion-N}(r)$						$g_{ion-H}(r)$					
ion	r_{M1}	r_{m1}	$n(r_{m1})$	r_{M2}	r_{m2}	$n(r_{m2})$	r_{M1}	r_{m1}	$n(r_{m1})$	r_{M2}	r_{m2}	$n(r_{m2})$
Li^+	2.25	2.83	4.0	5.03	6.2	25.7	2.79	3.43	14.1	5.39	6.68	92
Na^+	2.61	3.35	5.3	5.56	6.8	32.7	3.11	3.93	19.8	5.70	7.16	111
K^+	2.94	3.63	6.1	6.06	7.3	39.6	3.41	4.43	25.6	6.08	7.62	132
Rb^+	3.12	3.85	6.7	6.22	7.6	44.4	3.57	4.73	30.0	6.34	7.97	150
Cs^+	3.29	4.13	7.7	6.48	7.9	49.5	3.71	4.93	34.0	6.58	8.07	156

[a] r_{M1} and r_{M2} are the distances (Å), where the function has its first and second maximum, respectively. At r_{m1} and r_{m2} (in Å), the function has its first and second minimum. $n(r)$ represents the running integration numbers evaluated at $r = r_{m1}$ and r_{m2}.

Table 8. Average Numbers of NH_3 and H_2O Molecules in the First Solvation Shell of Alkali Cations in Aqueous Ammonia Solutions at 239.8 K and 1 atm[a]

	Li^+		Na^+		K^+		Rb^+		Cs^+	
x_{NH_3}	$n(NH_3)$	$n(H_2O)$	$n(NH_3)$	$n(H_2O)$	$n(NH_3)$	$n(H_2O)$	$n(NH_3)$	$n(H_2O)$	$n(NH_3)$	$n(H_2O)$
0.0	0 (0)	4 (20.2)	0 (0)	5.7 (24.0)	0 (0)	7.1 (26.8)	0 (0)	8.5 (28.5)	0 (0)	10.3 (29.0)
0.1	0 (2.2)	4 (17.6)	0.0 (2.0)	5.7 (21.9)	0.0 (1.8)	7.1 (25.6)	0.1 (1.7)	8.4 (27.7)	0.2 (1.7)	10.1 (27.1)
0.2	0 (4.1)	4 (15.3)	0.1 (3.8)	5.6 (19.7)	0.2 (4.0)	6.9 (22.9)	0.2 (4.0)	8.1 (24.7)	0.5 (3.7)	9.7 (24.4)
0.3	0 (6.0)	4 (13.0)	0.1 (6.1)	5.4 (16.9)	0.3 (6.5)	6.7 (19.8)	0.5 (6.6)	7.8 (21.4)	0.9 (5.7)	9.3 (21.7)
0.4	0 (8.3)	4 (10.3)	0.2 (8.1)	5.2 (14.3)	0.6 (8.9)	6.3 (16.6)	0.7 (8.8)	7.4 (18.6)	1.6 (8.5)	8.4 (18.0)
0.5	0 (9.6)	4 (8.7)	0.3 (10.4)	5.0 (11.3)	0.9 (11.3)	5.8 (13.6)	1.1 (11.6)	6.8 (15.0)	2.3 (11.0)	7.5 (14.8)
0.6	0 (11.5)	4 (6.6)	0.5 (12.4)	4.6 (8.7)	1.3 (13.7)	5.2 (10.4)	1.7 (14.3)	6.0 (11.4)	3.2 (14.4)	6.3 (11.5)
0.7	0 (12.2)	4 (5.8)	0.7 (13.8)	4.2 (6.7)	1.9 (15.5)	4.4 (7.8)	2.2 (16.2)	5.2 (8.8)	4.1 (15.4)	5.1 (8.6)
0.8	0 (12.8)	4 (4.8)	1.0 (14.6)	3.8 (5.3)	2.6 (16.7)	3.6 (5.9)	2.9 (17.5)	4.3 (6.5)	5.1 (17.1)	3.8 (5.8)
0.9	0 (13.3)	4 (4.4)	1.6 (15.3)	3.2 (3.8)	3.8 (17.8)	2.4 (3.5)	3.8 (18.6)	3.3 (4.4)	6.0 (18.3)	2.5 (3.5)
1.0	4 (25.7)	0 (0)	5.3 (32.7)	0 (0)	6.1 (39.6)	0 (0)	6.7 (44.4)	0 (0)	7.7 (49.5)	0 (0)

[a] The numbers of molecules in the first and second shells combined are reported within brackets.

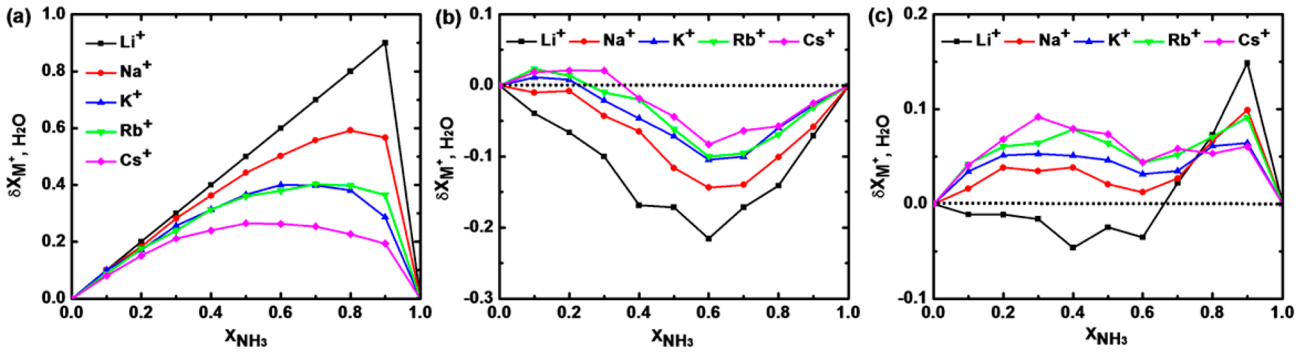

Figure 5. Preferential solvation by water of the first (a), second (b), and first plus second (c) solvation shells of alkali ions, $\delta x_{M^+,H_2O}$, as a function of the ammonia composition of the solution.

(more negative) than the corresponding hydration free energies of Tissandier et al.[66] (calculated using a similar cluster pair method).

3.5. Solvation Structure of Alkali Ions in Liquid Ammonia. The ion−ammonia Drude model is used to investigate the solvation structure of the alkali ions in liquid ammonia. For this purpose, systems composed of 250 NH_3 molecules and one alkali ion are simulated at 239.8 K and 1 atm for 20 ns. The structure of ammonia molecules around each ion is analyzed from the atom−atom correlation functions $g_{ion-N}(r)$ and $g_{ion-H}(r)$. The functions are calculated from the last 15 ns of each MD simulation and shown in Figure 4. Characteristics of the different functions are summarized in Table 7.

The $g_{ion-N}(r)$ function is characterized by a first peak that decreases in amplitude and shifts away from the ion on going from Li^+ to Cs^+. For lithium, the first minimum falls almost to zero, indicating that the first solvation shell is well structured and that exchange between ammonia molecules in the first and second solvation shells of Li^+ is rare. The analysis of the last 15 ns of a 20-ns simulation for the Li^+ system shows a minimum of 54 exchange events between molecules of the first and second solvation shells, which is large enough to ensure complete equilibration of the solvation structure. The coordination number up to the minimum of the first peak, which is the average number of ammonia molecules in the cation's first solvation shell, is 4.0 for Li^+, 5.3 for Na^+, 6.1 for K^+, 6.7 for Rb^+, and 7.7 for Cs^+ (see Table 7). The calculated coordination numbers for Li^+, Na^+, and Rb^+ are in good agreement with experimental estimates (4.0 for Li^+,[6,7,9] ~5.5 for Na^+,[6] and 6.4 for Rb^{8+}). To our knowledge, no experimental data are available for K^+ and Cs^+. Compared to our results, previous theoretical calculations have reported coordination numbers of 4[12,15,24] and 6[11,14,15,18,22] for Li^+; 5,[12,20] 7,[13] 8,[13,17,20] and 9[17] for Na^+; 8.7 for K^+;[16] and 10 for Cs^+.[12] This shows that, with the exception of previous theoretical

dx.doi.org/10.1021/ct4001069 | J. Chem. Theory Comput. 2013, 9, 2324−2338

investigations on Li^+,[12,15,25] the Drude model represents a significant improvement in describing the solvation structures. It should also be noted that some of the coordination numbers reported in the literature are calculated at higher temperatures (260[12] and 277 K[17,18]) and might be larger at the temperature considered in this work (239.8 K).

Compared to ammonia, the solvation of the alkali ions in SWM4-NDP water at 239.8 K and 1 atm shows coordination numbers of 4.0, 5.7, 7.1, 8.5, and 10.3 water molecules in the first solvation shell of Li^+, Na^+, K^+, Rb^+, and Cs^+, respectively. These numbers are obtained from MD simulations of one alkali ion in 250 water molecules, by integrating the $g_{ion-O}(r)$ function up to its first minimum (at 2.56 Å for Li^+, 3.24 Å for Na^+, 3.56 Å for K^+, 3.80 Å for Rb^+, and 4.10 Å for Cs^+). Except for Li^+, the coordination numbers are slightly larger at 239.8 K than at room temperature.[39] Except for Li^+, they are also higher than the equivalent numbers for ammonia, due to the smaller size of H_2O compared to NH_3.

3.6. Alkali Ions in Aqueous Ammonia. To investigate the preferential solvation of alkali ions in ammonia−water mixtures, simulations are performed on systems composed of a single alkali cation solvated by $(1 - x_{NH_3}) \times 250$ water molecules and $x_{NH_3} \times 250$ ammonia molecules, with x_{NH_3} ranging from 0 to 1. Each simulation is run for 70 ns, and the analysis is based on the last 65 ns.

Table 8 reports the number of ammonia and water molecules in the first and first plus second solvation shells of each cation. These coordination numbers are calculated by integrating the $g_{ion-N}(r)$ and $g_{ion-O}(r)$ RDFs up to the minimum following the first (or second) peak in the total, $g_{ion-(N+O)}(r)$ RDF. The positions of these minima are weakly dependent on the mixture composition, with the first minimum at 2.80 Å for Li^+, 3.18 Å for Na^+, 3.56 Å for K^+, 3.80 Å for Rb^+, and 4.10 Å for Cs^+ and the second minimum at 5.06 Å for Li^+, 5.40 Å for Na^+, 5.74 Å for K^+, and 5.90 Å for both Rb^+ and Cs^+. For pure solvents (x_{NH_3} = 0 or 1), integration is performed up to the first and second minima of $g_{ion-O}(r)$ and $g_{ion-N}(r)$ RDFs. (The second minimum in the $g_{ion-O}(r)$ function is at 5.06 Å for Li^+, 5.40 Å for Na^+, 5.67 Å for K^+, 5.80 Å for Rb^+, and 5.88 Å for Cs^+; the first minima are reported in section 3.5.)

Preferential solvation of the ions is monitored using the following parameter:[67]

$$\delta x_{M^+,H_2O} = x^{local}_{M^+,H_2O} - x_{H_2O} = x_{NH_3} - x^{local}_{M^+,NH_3} \quad (7)$$

where $x^{local}_{M^+,H_2O}$ and $x^{local}_{M^+,NH_3}$ represent the local mole fractions of water and ammonia in the first, second, or first plus second solvation shells of the ion, and x_{H_2O} and x_{NH_3} are the bulk mole fractions of water and ammonia.[67] Figure 5 shows the preferential water solvation of the various solvation shells of each ion as a function of x_{NH_3}.

The positive sign of $\delta x_{M^+,H_2O}$ in the first solvation shell (Figure 5a) indicates that alkali ions are preferentially solvated by water over the entire composition range. For any given composition, the preferential hydration follows the trend $Li^+ > Na^+ > K^+ \approx Rb^+ > Cs^+$. For Li^+, $\delta x_{M^+,H_2O}$ is exactly equal to x_{NH_3} up to x_{NH_3} = 0.9 because the occupancy of NH_3 in the first solvation shell is too low to be sampled from free MD simulations (given the slow rate of exchange of molecules around lithium).

The number of ammonia and water molecules in the second solvation shells is calculated from the numbers in the first shell and in the first and second shells combined (see Table 8). Counterbalancing the first solvation shell, the second shell is more favorably occupied by ammonia than by water, as evidenced by the negative values of $\delta x_{M^+,H_2O}$ for all ions over most of the composition range (see Figure 5b). The preferential solvation in the second solvation shell follows for NH_3 molecules the same trend it follows for H_2O molecules in the first solvation shell ($Li^+ > Na^+ > K^+ \approx Rb^+ > Cs^+$).

Because of the complementary affinities of the first and second shells, the two shells combined display no marked solvation preference for either water or ammonia (see Figure 5c).

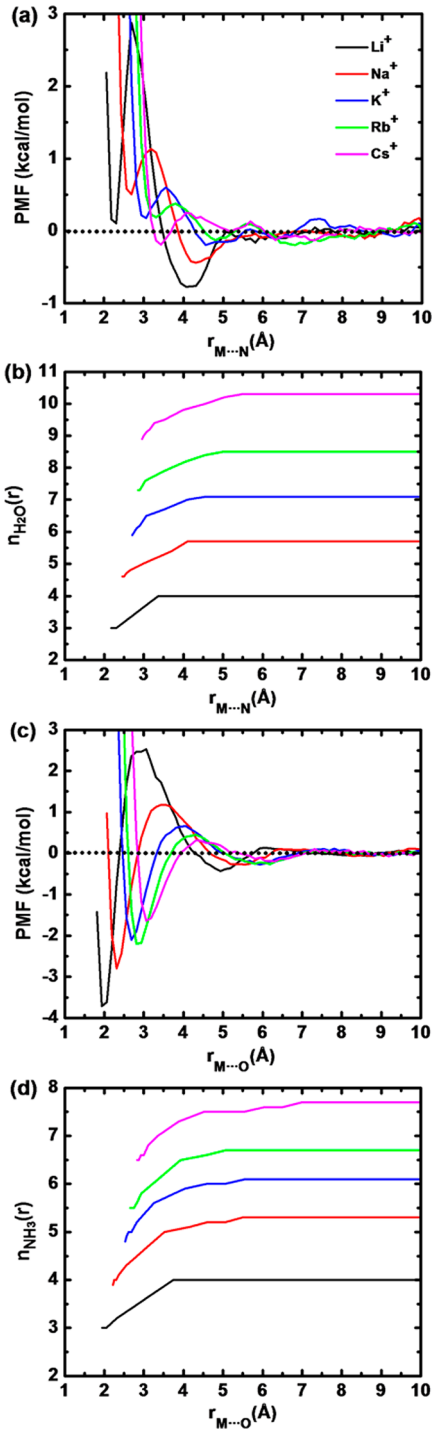

Figure 6. PMFs between alkali ions and an ammonia molecule in liquid water (a) and between alkali ions and a water molecule in liquid ammonia (c). The number of first-shell solvent molecules are shown in panels (b) and (d). Colors are as per panel a.

dx.doi.org/10.1021/ct4001069 | J. Chem. Theory Comput. 2013, 9, 2324−2338

Table 9. Properties of the PMFs between Alkali Ions and NH_3 in Water and between the Ions and H_2O in Ammonia, Calculated at T = 239.8 K and p = 1 atm[a]

	1 NH_3 in 250 H_2O					1 H_2O in 250 NH_3				
property	Li^+	Na^+	K^+	Rb^+	Cs^+	Li^+	Na^+	K^+	Rb^+	Cs^+
r_{m1}	2.27	2.66	3.03	3.30	3.43	2.00	2.34	2.72	2.88	3.12
PMF(r_{m1})	0.1	0.5	0.2	0.2	−0.2	−3.7	−2.8	−2.1	−2.2	−1.6
n_1	3.0	4.8	6.4	7.8	9.4	3.0	4.1	5.0	5.7	6.8
Δn_1	−1.0	−0.9	−0.7	−0.7	−0.9	−1.0	−1.2	−1.1	−1.0	−0.9
r_{m2}	4.1	4.3	4.6	4.8	5.2	4.9	5.5	5.9	6.2	6.3
PMF(r_{m2})	−0.8	−0.4	0.0	0.0	0.0	−0.4	−0.3	−0.3	−0.3	−0.2
n_2	4.0	5.7	7.1	8.4	10.2	4.0	5.3	6.1	6.7	7.6
Δn_2	−0.0	−0.0	−0.0	−0.1	−0.1	−0.0	−0.0	−0.0	−0.0	−0.1

[a] r_{m1} and r_{m2} are ion−ligand distances (in Å) at which the PMF (in kcal/mol) possesses a minimum. n_1 and n_2 are numbers of first-shell solvent molecules at $r = r_{m1}$ and r_{m2}. Δn_1 and Δn_2 are numbers of first-shell solvent molecules displaced by ligand complexation at r_{m1} and r_{m2}.

Over the first two solvation shells, Li^+ shows slight preferential solvation by NH_3 for $x_{NH_3} < 0.7$, while Na^+, K^+, Rb^+, and Cs^+ show slight preferential solvation by water over the entire concentration range.

In aqueous ammonia solutions, alkali ions can therefore be viewed as water-selective in their first shells, ammonia-selective in their second shells, and, except for Li^+, slightly water-selective over both shells. Since the ion−ammonia dimer in the gas phase has a greater binding energy than the ion−water dimer (see section 3.1.1), preferential solvation of the ions by ammonia might have been expected. Preferential solvation by water, however, could be attributed to the following two factors: (1) The smaller size of water relative to ammonia results in larger water coordination numbers (see Table 8) and in larger water clusters being more stable than the corresponding ammonia clusters. (2) Water molecules in the first solvation shell form strong O−H···N and O−H···O hydrogen bonds with ammonia and water molecules in the second solvation shell, while first-shell ammonia molecules form weak N−H···N and N−H···O hydrogen bonds.

Previous classical simulations on a single Li^+, Na^+, or K^+ solvated in 18.4% ammonia molar fraction have shown the following compositions for the first and second shells (using the notation "ion[first shell][second shell]"): $Li^+[(H_2O)_4(NH_3)_2][(H_2O)_8(NH_3)_4]$,[31] $Li^+[(H_2O)_3(NH_3)_3]$,[32] $Na^+[(H_2O)_{2.4}(NH_3)_4][(H_2O)_7(NH_3)_2]$,[30] $Na^+[(H_2O)_{4.9}(NH_3)_{2.2}]$,[33] and $K^+[(H_2O)_{5.3}(NH_3)_{3.4}]$.[34] QM/MM simulations of the same system show $Li^+[(H_2O)_3(NH_3)][(H_2O)_4(NH_3)_2]$,[32,35] $Li^+[(H_2O)_4][(H_2O)_4]$,[35] $Na^+[(H_2O)_{3.7}(NH_3)_{1.8}]$,[33] and $K^+[(H_2O)_{6.7}(NH_3)_{0.9}]$.[34] These QM/MM simulations have been performed using a QM region that includes either only the first solvation shell of the ion[32−34] or both the first and second solvation shells.[35] While QM/MM simulation results are expected to be more reliable, some of the structures they predict are questionable. First, it appears that the solvation structure is highly dependent on the size of the QM region.[35] Second, according to the hard−soft acid−base theory, the hardness of the alkali ions decreases as the ion size increases and therefore should favor complexation with the softer base (NH_3). The QM/MM simulations of Tongraar and Rode[33−35] show affinities toward NH_3 following the trend $Na^+ > K^+ > Li^+$, inconsistent with the expected trend ($K^+ > Na^+ > Li^+$). By contrast, the Drude model shows the expected behavior: Larger ions have higher ammonia affinities (see Table 8 and Figure 5a). Ab initio MD simulations of a neutral Li atom in 20 water and six ammonia molecules[36] have shown ionization of Li and preferential coordination by four water molecules, in agreement with our results.

On the basis of the solvation structures reported for Li^+ and Na^+ from MC simulations,[30,31] we calculate a $\delta x_{M^+,H_2O}$ value of −0.15 for both shells of Li^+ and of −0.44 and −0.04 for the first and second shells of Na^+, respectively. Such preferential first-shell solvation by ammonia is at odds with the hardnesses of the two ions. The more recent QM/MM investigation of Li^+ solvation in 18.4% aqueous ammonia by Tongraar and Rode[35] shows a preferential hydration parameter of +0.184 for both solvation shells. While the preferential hydration of the first shell is consistent with our findings, Tongraar and Rode report that the Li^+ ion's second shell is populated by only about four molecules,[35] compared to 15.4 molecules from our simulations at 20% ammonia and 12.0 molecules from previous MC simulations.[31]

To further analyze the affinity of each solvent component for the ions, we calculate the PMF of association of an ion to a single NH_3 molecule in liquid water (see Figure 6a) and of an ion to a single H_2O molecule in liquid ammonia (see Figure 6c). These PMFs are computed under the thermodynamic conditions used to investigate preferential solvation (T = 239.8 K, p = 1 atm). Figure 6 also displays the number of first-shell solvent molecules as a function of the ion−ligand distance, which describes the influence of the ligand on first-shell solvent occupancy. Table 9 reports r_{m1} and r_{m2}, the ion−ligand distances corresponding respectively to the first- and second-shell PMF minima; n_1 and n_2, the numbers of first-shell solvent molecules when the ligand is respectively at distances r_{m1} and r_{m2} from the ion; as well as Δn_1 and Δn_2, the numbers of first-shell solvent molecules displaced when the ligand is at distances r_{m1} and r_{m2}. The coordination numbers are calculated from the pair distribution functions g_{ion-O} and g_{ion-N} up to their first minimum.

Figure 6a and Table 9 show that, while NH_3 binds the first solvation shell only for Cs^+ (PMF(r_{m1}) < 0), it mainly binds the second solvation shell only for Li^+ and Na^+ (PMF(r_{m2}) < 0). This is consistent with the "second-shell" values of $\delta x_{M^+,H_2O}$ when x_{NH_3} is close to 0 (see Figure 5b): In dilute NH_3 aqueous solutions, $\delta x_{M^+,H_2O}$ is positive for K^+, Rb^+, and Cs^+ but negative for Li^+ and Na^+. Table 9 also shows that, while binding of NH_3 in the first solvation shell results in the displacement of at least 0.7 first-shell water molecules, binding in the second shell causes a depletion of no more than 0.1 first-shell molecules, indicating that the presence of NH_3 in the second shell does not significantly perturb the hydration structure.

In contrast to NH_3 in water, H_2O in ammonia shows a high affinity for the ion's first solvation shell that follows the trend $Li^+ > Na^+ > K^+ \approx Rb^+ > Cs^+$ (see Figure 6c and Table 9).

This infinite-dilution result is consistent with the observed trend in preferential hydration over the entire composition range (see Figure 5a). The shallow minimum at 5−6 Å distances corresponds to solvent-separated pairs.

4. CONCLUSION

A polarizable model based on classical Drude oscillators is optimized for alkali ion−ammonia interactions based on the ab initio properties of the individual dimers. The model gives binding energies for larger ion−ammonia and ion−ammonia−water clusters in very good agreement with ab initio MP2 results, gives relative solvation free energies of ions in liquid ammonia in good agreement with experiments, and yields structures of ammonia-solvated ions in very good agreement with experimental structures. It also reproduces binding cooperativity in ion−ammonia and ion−ammonia−water clusters, an effect that cannot be captured by pairwise-additive force fields. The model is used to investigate the preferential solvation of alkali ions in aqueous ammonia solutions and shows preferential binding for water in the first solvation shell and for ammonia in the second solvation shell.

In the present work, water−ammonia mixtures were used as a prototypical system to analyze ligand competition in the first and second coordination shells of metal ions. The concepts developed in this work will likely be applicable to preferential solvation involving more complex ligands. They will also likely help in rationalizing ion selectivity and ion coordination in biological molecules such as proteins and nucleic acids.

AUTHOR INFORMATION

Corresponding Author

*Tel.: +1-514-848-2424, extension 5314. Fax: +1-514-848-2868. E-mail: guillaume.lamoureux@concordia.ca.

Notes

The authors declare no competing financial interest.

†On leave from Department of Chemistry, Faculty of Science, Assiut University, Assiut 71516, Egypt

ACKNOWLEDGMENTS

This work was supported in part by an FQRNT Nouveaux chercheurs grant and an NSERC Discovery grant to G.L. and by a PROTEO scholarship, a GEPROM scholarship, a Garnet Strong scholarship, and a Power Corporation of Canada graduate fellowship to E.A.O. Computational resources were provided by Calcul Québec.

REFERENCES

(1) Appl, M. Ammonia, 1. Introduction. In *Ullmann's Encyclopedia of Industrial Chemistry*; Wiley-VCH: Weinheim, Germany, 2011.
(2) Kraus, C. A.; Lucasse, W. W. *J. Am. Chem. Soc.* **1921**, *43*, 2529−2539.
(3) Kraus, C. A.; Carney, E. S.; Johnson, W. C. *J. Am. Chem. Soc.* **1927**, *49*, 2206−2213.
(4) Johnson, W. C.; Meyer, A. W. *J. Am. Chem. Soc.* **1932**, *54*, 3621−3628.
(5) Wasse, J. C.; Hayama, S.; Neal T. Skipper, N. T. *Phys. Rev. B* **2000**, *61*, 11993−11997.
(6) Wasse, J. C.; Hayama, S.; Masmanidis, S.; Stebbings, S. L.; Skipper, N. T. *J. Chem. Phys.* **2003**, *118*, 7486−7494.
(7) Thompson, H.; Wasse, J. C.; Skipper, N. T.; Hayama, S.; Bowron, D. T.; Sope, A. K. *J. Am. Chem. Soc.* **2003**, *125*, 2572−2581.
(8) Wasse, J. C.; Hayama, S.; Skipper, N. T. *J. Phys. Chem. B* **2003**, *107*, 14452−14456.
(9) Thompson, H.; Wasse, J. C.; Skipper, N. T.; Howard, C. A.; Bowron, D. T.; Soper, A. K. *J. Phys.: Condens. Matter* **2004**, *16*, 5639−5652.
(10) Salter, T. E.; Mikhailov, V.; Ellis, A. M. *J. Phys. Chem. A* **2007**, *111*, 8344−8351.
(11) Hannongbua, S.; Ishida, T.; Spohr, E.; Heinzinger, K. *Z. Naturforsch. A* **1988**, *43*, 572−582.
(12) Marchi, M.; Sprik, M.; Klein, M. L. *J. Phys.: Condens. Matter* **1990**, *2*, 5833−5848.
(13) Hannongbua, S. *Aust. J. Chem.* **1991**, *44*, 447−456.
(14) Gurskii, Z.; Hannongbua, S.; Heinzinger, K. *Mol. Phys.* **1993**, *78*, 461−474.
(15) Kerdcharoen, T.; Liedl, K. R.; Rode, B. M. *Chem. Phys.* **1996**, *211*, 313−323.
(16) Tongraar, A.; Hannongbua, S.; Rode, B. M. *Chem. Phys.* **1997**, *219*, 279−29.
(17) Hannongbua, S. *J. Chem. Phys.* **1997**, *106*, 6076−6081.
(18) Hannongbua, S. *Chem. Phys. Lett.* **1998**, *288*, 663−668.
(19) Kerdcharoen, T.; Hannongbua, S. *Chem. Phys. Lett.* **1999**, *310*, 333−341.
(20) Kerdcharoen, T.; Rode, B. M. *J. Phys. Chem. A* **2000**, *104*, 7073−7078.
(21) Mierzwicki, K.; Latajka, Z. *Chem. Phys.* **2001**, *265*, 301−311.
(22) Hannongbua, S.; Remsungnen, T.; Kiselev, M.; Heinzinger, K. *Condens. Matter Phys.* **2003**, *6*, 459−470.
(23) Corral, I.; Mó, O.; Yáñez, M.; Radom, L. *J. Phys. Chem. A* **2005**, *109*, 6735−6742.
(24) Salter, T. E.; Ellis, A. M. *Chem. Phys.* **2007**, *332*, 132−138.
(25) Chandra, A.; Marx, D. *Angew. Chem., Int. Ed.* **2007**, *46*, 3676−3679.
(26) Lim, I. S.; Botschwina, P.; Oswald, R.; Barone, V.; Stoll, H.; Schwerdtfeger, P. *J. Chem. Phys.* **2007**, *127*, 104313-1−104313-12.
(27) Pinsook, U.; Scheicher, R. H.; Ahuja, R.; Hannongbua, S. *J. Phys. Chem. A* **2008**, *112*, 5323−5326.
(28) Almeida, T. S.; Cabral, B. J. C. *J. Chem. Phys.* **2010**, *132*, 094307-1−094307-10.
(29) Tongraar, A.; Hannongbua, S. *J. Phys. Chem. B* **2008**, *112*, 885−891.
(30) Rode, B. M.; Tanabe, Y. *J. Chem. Soc., Faraday Trans. 2* **1988**, *84*, 1779−1788.
(31) Kheawsrikul, S.; Hannongbua, S. V.; Kokpol, S. U.; Rode, B. M. *J. Chem. Soc., Faraday Trans. 2* **1989**, *85*, 643−649.
(32) Tongraar, A.; Rode, B. M. *J. Phys. Chem. A* **1999**, *103*, 8524−8527.
(33) Tongraar, A.; Rode, B. M. *J. Phys. Chem. A* **2001**, *105*, 506−510.
(34) Tongraar, A.; Rode, B. M. *Phys. Chem. Chem. Phys.* **2004**, *6*, 411−416.
(35) Tongraar, A.; Rode, B. M. *Chem. Phys. Lett.* **2008**, *466*, 61−64.
(36) Pratihar, S.; Chandra, A. *J. Chem. Phys.* **2011**, *134*, 024519−1−024519−8.
(37) Glendening, E. D. *J. Am. Chem. Soc.* **1996**, *118*, 2473−2482.
(38) Lamoureux, G.; Harder, E.; Vorobyov, I.; Roux, B.; MacKerell, A. D. *Chem. Phys. Lett.* **2006**, *418*, 245−249.
(39) Yu, H.; Whitfield, T.; Harder, E.; Lamoureux, G.; Vorobyov, I.; Anisimov, V. M.; MacKerell, A. D.; Roux, B. *J. Chem. Theory Comput.* **2010**, *6*, 774−786.
(40) Frisch, M. J.; Trucks, G. W.; Schlegel, H. B.; Scuseria, G. E.; Robb, M. A.; Cheeseman, J. R.; Scalmani, G.; Barone, V.; Mennucci, B.; Petersson, G. A.; Nakatsuji, H.; Caricato, M.; Li, X.; Hratchian, H. P.; Izmaylov, A. F.; Bloino, J.; Zheng, G.; Sonnenberg, J. L.; Hada, M.; Ehara, M.; Toyota, K.; Fukuda, R.; Hasegawa, J.; Ishida, M.; Nakajima, T.; Honda, Y.; Kitao, O.; Nakai, H.; Vreven, T.; Montgomery, J. A., Jr.; Peralta, J. E.; Ogliaro, F.; Bearpark, M.; Heyd, J. J.; Brothers, E.; Kudin, K. N.; Staroverov, V. N.; Kobayashi, R.; Normand, J.; Raghavachari, K.; Rendell, A.; Burant, J. C.; Iyengar, S. S.; Tomasi, J.; Cossi, M.; Rega, N.; Millam, J. M.; Klene, M.; Knox, J. E.; Cross, J. B.; Bakken, V.; Adamo, C.; Jaramillo, J.; Gomperts, R.; Stratmann, R. E.; Yazyev, O.; Austin, A. J.; Cammi, R.; Pomelli, C.; Ochterski, J. W.; Martin, R. L.; Morokuma, K.; Zakrzewski, V. G.; Voth, G. A.; Salvador, P.;

Dannenberg, J. J.; Dapprich, S.; Daniels, A. D.; Farkas, Ö.; Foresman, J. B.; Ortiz, J. V.; Cioslowski, J.; Fox, D. J. *Gaussian 09*, revision B.01; Gaussian, Inc.: Wallingford, CT, 2009.
(41) The Stuttgart relativistic small core basis set was obtained from EMSL Basis Set Library at the URL https://bse.pnl.gov/bse/portal. For the original valence basis set and ECP reference, see: Bergner, A.; Dolg, M.; Kuechle, W.; Stoll, H.; Preuss, H. *Mol. Phys.* **1993**, *80*, 1431−1441.
(42) Coletti, C.; Re, N. *J. Phys. Chem. A* **2006**, *110*, 6563−6570.
(43) Boys, S. F.; Bernardi, F. *Mol. Phys.* **1970**, *19*, 553−566.
(44) Orabi, E. A.; Lamoureux, G. *J. Chem. Theory Comput.* **2013**, *9*, 2035−2051.
(45) Brooks, B. R.; Brooks, C. L.; Mackerell, A. D.; Nilsson, L.; Petrella, R. J.; Roux, B.; Won, Y.; Archontis, G.; Bartels, C.; Boresch, S.; Caflisch, A.; Caves, L.; Cui, Q.; Dinner, A. R.; Feig, M.; Fischer, S.; Gao, J.; Hodoscek, M.; Im, W.; Kuczera, K.; Lazaridis, T.; Ma, J.; Ovchinnikov, V.; Paci, E.; Pastor, R. W.; Post, C. B.; Pu, J. Z.; Schaefer, M.; Tidor, B.; Venable, R. M.; Woodcock, H. L.; Wu, X.; Yang, W.; York, D. M.; Karplus, M. *J. Comput. Chem.* **2009**, *30*, 1545−1614.
(46) Lamoureux, G.; Roux, B. *J. Chem. Phys.* **2003**, *119*, 3025−3039.
(47) Orabi, E. A.; Lamoureux, G. *J. Chem. Theory Comput.* **2012**, *8*, 182−193.
(48) Lamoureux, G.; Orabi, E. A. *Mol. Simul.* **2012**, *38*, 704−722.
(49) Wang, S.; Orabi, E. A.; Baday, S.; Bernèche, S.; Lamoureux, G. *J. Am. Chem. Soc.* **2012**, *134*, 10419−10427.
(50) Martyna, G. J.; Tuckerman, M. E.; Tobias, D. J.; Klein, M. L. *Mol. Phys.* **1996**, *87*, 1117−1157.
(51) Essmann, U.; Perera, L.; Berkowitz, M. L.; Darden, T.; Lee, H.; Pedersen, L. G. *J. Chem. Phys.* **1995**, *103*, 8577−8593.
(52) Lagüe, P.; Pastor, R. W.; Brooks, B. R. *J. Phys. Chem. B* **2004**, *108*, 363−368.
(53) Deng, Y.; Roux, B. *J. Phys. Chem. B* **2004**, *108*, 16567−16576.
(54) Lamoureux, G.; Roux, B. *J. Phys. Chem. B* **2006**, *110*, 3308−3322.
(55) Kumar, S.; Bouzida, D.; Swendsen, R. H.; Kollman, P. A.; Rosenberg, J. M. *J. Comput. Chem.* **1992**, *13*, 1011−1021.
(56) Souaille, M.; Roux, B. *Comput. Phys. Commun.* **2001**, *135*, 40−57.
(57) Woodin, R. L.; Beauchamp, J. L. *J. Am. Chem. Soc.* **1978**, *100*, 501−508.
(58) Armentrout, P. B.; Rodgers, M. T. *J. Phys. Chem. A* **2000**, *104*, 2238−2247.
(59) Iceman, C.; Armentrout, P. *Int. J. Mass Spectrom.* **2003**, *222*, 329−349.
(60) Džidić, I.; Kebarle, P. *J. Phys. Chem.* **1970**, *74*, 1466−1474.
(61) Glendening, E. D.; Feller, D. *J. Phys. Chem.* **1995**, *99*, 3060−3067.
(62) Lamoureux, G.; MacKerell, A. D.; Roux, B. *J. Chem. Phys.* **2003**, *119*, 5185−5197.
(63) Halgren, T. A. *J. Am. Chem. Soc.* **1992**, *114*, 7827−7843.
(64) Plambeck, J. A. *Can. J. Chem.* **1969**, *47*, 1401−1410.
(65) Tuttle, T. R.; Malaxos, S.; Coe, J. V. *J. Phys. Chem. A* **2002**, *106*, 925−932.
(66) Tissandier, M. D.; Cowen, K. A.; Feng, W. Y.; Gundlach, E.; Cohen, M. H.; Earhart, A. D.; Coe, J. V. *J. Phys. Chem. A* **1998**, *102*, 7787−7794.
(67) Marcus, Y. *J. Chem. Soc., Faraday Trans. 1* **1988**, *84*, 1465−1473.